University of Alberta
Department of Civil Engineering

Structural Engineering Report No. 60

The Second-Order Analysis and Design of Reinforced Concrete Frames

by

G.S. Mathews

and

J.G MacGregor

January, 1977

THE SECOND-ORDER ANALYSIS AND DESIGN OF REINFORCED CONCRETE FRAMES

BY

GREGORY STANLEY MATHEWS

JAMES G. MACGREGOR

The University of Alberta
Department of Civil Engineering
Edmonton, Alberta, Canada

January, 1977

ABSTRACT

Three approximate methods of second-order analysis are compared to an "exact" second-order analysis. They are the Fey method, the moment magnifier method and the amplified lateral load method.

In general, the Fey method and the moment magnifier method are shown to give good approximations with a slight degree of conservatism. The amplified lateral load method is shown to be very conservative in the more flexible frames studied.

Column design following a second-order analysis is also presented. It is shown that estimating the maximum design moment within a column is underestimated when the calculations are based on the braced frame effective length and that an effective length equal to the actual length should be used.

ACKNOWLEDGEMENTS

This study was made possible by a grant provided by the National Research Council of Canada

The author wishes to thank Dr. J.G. MacGregor for his invaluable guidance on this thesis.

TABLE OF CONTENTS

LIST OF TABLES

LIST OF FIGURES

FIGURE	DESCRIPTION	PAGE
4.8	Moment Errors in Frame Type Seven	51
4.9	Moment Errors in Frame Type Eight	52
4.10	Moment Errors in Frame Type Nine	53
4.11	Moment Errors in Frame Type Ten	54
4.12	Moment Errors in Frame Type Eleven	55
5.1	Forces in Deflected Column	57
5.2	Limits on Columns with Maximum Moment at End of Column	60
5.3	Test Frame	62
5.4	Deflections and Moments in Windward Column	64
A.1	Frame Type One	73
A.2	Frame Type Two	74
A.3	Frame Type Three	75
A.4	Frame Type Four	76
A.5	Frame Type Five	77
A.6(a)	Frame Type Six	78
A.6(b)	Frame Type Six	79
A.7(a)	Frame Type Seven	80
A.7(b)	Frame Type Seven	81
A.8	Frame Type Eight	82
A.9	Frame Type Nine	83
A.10	Frame Type Ten	84
A.11	Frame Type Eleven	85

NOTATION

A	=	cross-sectional area of bracing member
E	=	modulus of elasticity
h	=	storey or building height
H	=	shear in a given storey
H_s	=	service storey shear
H_u	=	ultimate storey shear
I	=	moment of inertia
K_ℓ	=	H/Δ_1 = lateral stiffness
K	=	effective length factor
L	=	length of column, center to center of joints
L_o	=	length of brace
M_1	=	first-order moment
M_2	=	total second-order moment = first-order moment plus P-Δ effect
M_a	=	larger end moment in a column, always positive
M_b	=	smaller end moment in a column, positive if column is bent in single curvature
P	=	axial load in a column
P_{cr}	=	critical load of a column in a storey or frame in lateral buckling
P_E	=	π^2EI/L^2 = Euler buckling load
P_u	=	ultimate load in a column
Q	=	$\Sigma P\Delta_1/Hh$ = stability index
α	=	hP/EI, $\alpha^2 = \pi^2(P/P_E)$
β	=	slope of brace in Figure 2.4(b)

δ = moment magnifier

Δ_1 = first-order deflection

Δ_2 = $\Delta_1 + \Delta_a$ = total second-order deflection

Δ_a = additional deflection due to P-Δ effect

ψ = Δ/h = storey drift

CHAPTER I

INTRODUCTION

1.1 What Problem Is

Design of a reinforced concrete frame is preceeded by a structural analysis to determine member end forces and moments. The analysis is usually effected by a computer program based on the direct stiffness method. The majority of such programs assume linear elastic behavior of all members and are first-order programs, that is, equilibrium is formulated on the undeformed structure. While the assumption of elastic behavior is reasonable for a structure under working loads, the neglect of the effects of deformations represents a greater restriction, especially in flexible structures subjected to lateral and vertical loads.

An analysis which formulates equilibrium on the deformed structure is called a second-order analysis. If the lateral deflections of the isolated storey shown in Figure 1.1 are ignored equilibrium could be written as:

$$\Sigma M = M_1 + M_2 + M_3 + M_4 = Hh \qquad 1.1$$

Had equilibrium been formulated on the deformed storey (second-order solution), Equation 1.1 would have appeared as:

$$\Sigma M = M_1 + M_2 + M_3 + M_4 = Hh + P\Delta_2 \qquad 1.2$$

The first-order solution ignores the term $P\Delta_2$. It should also be noted that the deflections computed in a first-order analysis, Δ_1, are less than those of a second-order analysis, Δ_2.

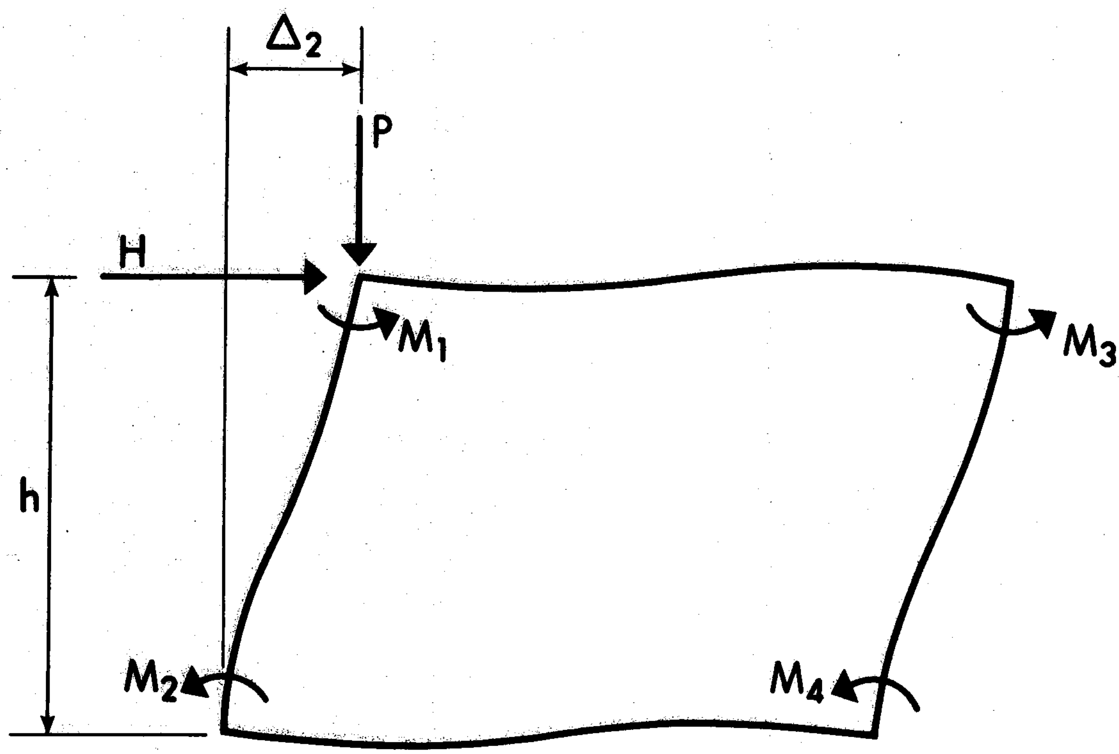

FIGURE 1.1 DEFORMED STOREY UNDER COMBINED LOADING

1.2 Scope of Thesis

Due to the cause and effect nature of the P-Δ phenomenon, the determination of the second-order deflections is frequently done in an iterative computation which can be tedious.

The intent of this thesis is to review and compare several approximate procedures which obviate the need to perform successive iterations. Design rules based on these analyses are also verified.

Chapter two presents a review of frame stability and second-order effects in frames. A series of eleven frames used to compare the analyses are described in Chapter three. Chapter four discusses the approximate methods of analysis and compares the results of these analyses to those from an "exact" analysis. Chapter five considers the column design procedures which are necessary once a second-order analysis has been carried out.

CHAPTER 2

BACKGROUND INFORMATION

2.1 Introduction

This chapter presents a brief review of frame stability by considering slenderness effects in buildings. A number of methods of second-order analysis are outlined[1,3,4,10].

2.2 Frame Stability

2.2.1 Frame Response to Horizontal and Vertical Loads

The material in this section is based on Reference 10. Similar analyses have been presented by Stevens[16], Fey[17], Goldberg[18] and Parme[19].

Figure 2.1(a) represents a storey in a frame subjected to combined loading. Let Δ_1 denote the relative deflection between the top and bottom floors of the given storey as a result of lateral forces only. The corresponding storey stiffness may then be defined as $K_\ell = H/\Delta_1$ in which H is the storey shear.

Application of the vertical loads will tend to increase the relative lateral deflection by an amount Δ_a. The total relative deflection, Δ_2, is then the sum of Δ_1 and Δ_a. The total storey moment (sum of top and bottom end moments in all the columns) will be

$$M_2 = Hh + \Sigma P\Delta_2 \qquad 2.1$$

in which h is the storey height and ΣP is the sum of applied vertical loads down to the storey considered. If it is assumed that the moment diagrams in the columns resulting from the action of the vertical loads

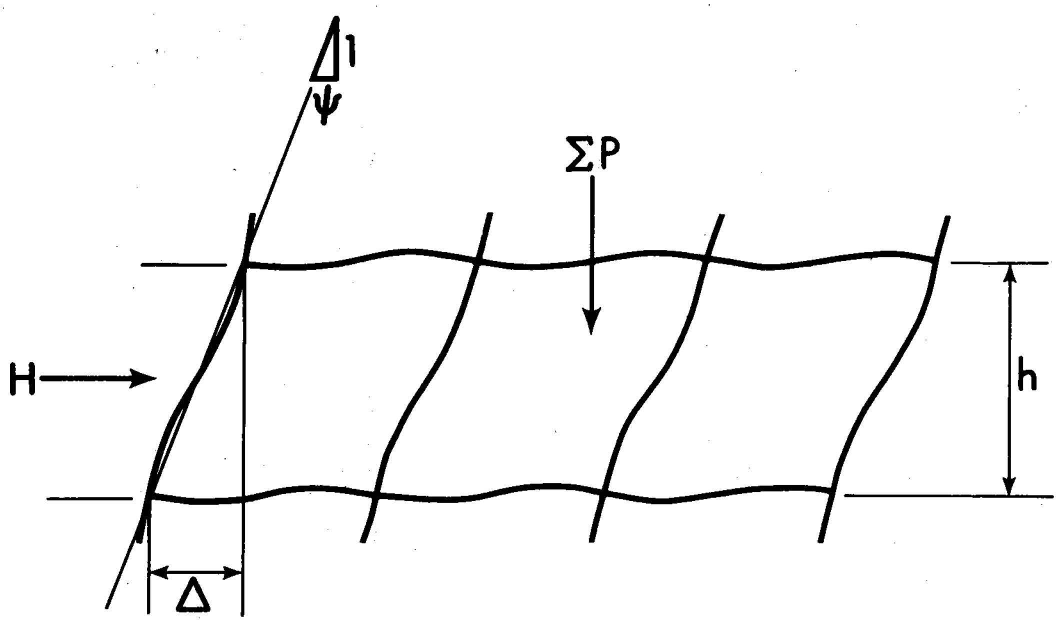

FIGURE 2.1(a) STOREY UNDER COMBINED LOAD

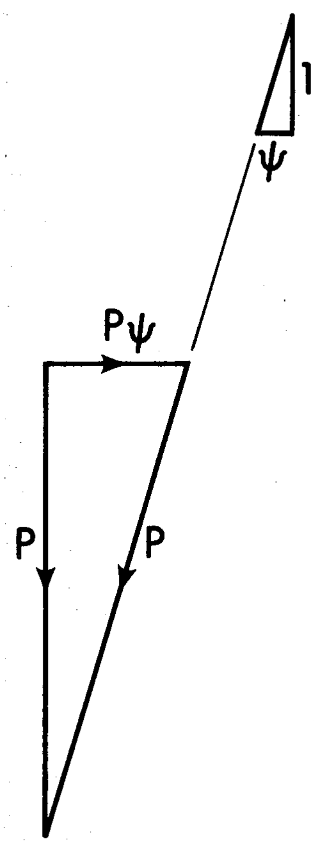

FIGURE 2.1(b) DECOMPOSITION OF VERTICAL LOAD

have the same shape as those produced by the lateral forces, which will be essentially true if the columns are stiffer than the beams. The storey moments can be taken equal to $hK_\ell\Delta_2$. Equation 2.1 then gives

$$\Delta_2 = \frac{H}{K_\ell - \frac{\Sigma P}{h}} \qquad 2.2$$

and,

$$M_2 = Hh\left[1 + \frac{\frac{\Sigma P}{h}}{K_\ell - \frac{\Sigma P}{h}}\right] \qquad 2.3$$

Hence, slenderness effects are taken into account by introducing a magnification factor given by Equation 2.3 that multiplies the nominal storey moment Hh. Reference 2 proposes that all stresses and deformations resulting from the sole action of the lateral forces be multiplied by the same factor.

Approximate proportionality of the bending moment diagrams in columns, as a result of lateral and vertical forces, requires that the columns in every storey deflect as nearly straight lines and that Δ_2 be nearly proportional to Δ in all the storeys, so that the storey shear stiffness remains practically constant.

Considering again the deformed storey of Fig. 2.1(a), if axial deformation and higher order terms are neglected, all joints in a floor will remain in a horizontal plane as the frame deflects. The storey drift is defined as $\psi = \Delta/h$ and is the same for all the columns in a given storey. The load P is now replaced by its horizontal and inclined components as in Fig. 2.1(b).

The horizontal component is equal to $P\psi$ while the second is essentially equal to P for small drifts and columns deflecting as straight lines. Consequently, the combined action of vertical loads and an applied storey shear, H, on the deflected frame is equivalent to the action of the original axial loads on the columns, combined with an increased storey shear, $H + P\psi$, as given by Equation 2.1.

If the beams are rigid in comparison with the columns, the columns will not deflect as straight lines. Consider the case of infinitely rigid beams and the coordinate system of Figure 2.2. Let $\Delta(y)$ denote the deflections of a column, as a result of the storey shear alone. For a small axial load P, the bending moment increases by $P\Delta$. The deflection of the top relative to the bottom, due to P, is found to be $P\Delta h^2/9.87\ EI$ assuming the column deflects as a sine wave. Therefore, the increased lateral deflection due to the vertical load is:

$$\Delta_a = \left[\Delta_1 + \Delta_a\right] \frac{Ph^2}{9.87\ EI} \qquad 2.4$$

But the lateral stiffness K_ℓ due to lateral loads only is $K_\ell = 12(\Sigma EI)/h^3$, where the sum extends to all the columns in a storey considered. From Equation 2.4 then,

$$\Delta_a = \left[\frac{H}{K_\ell} + \Delta_a\right] \frac{1.22\ \Sigma P}{K_\ell h} \qquad 2.5$$

$$\Delta_2 = \frac{H}{K_\ell - \dfrac{1.22\ \Sigma P}{h}} \qquad 2.6$$

and,

$$M_2 = Hh \left[1 + \frac{\dfrac{\Sigma P}{h}}{K_\ell - \dfrac{1.22\ \Sigma P}{h}}\right] \qquad 2.7$$

The term 1.22 will vary from 1.0 to 1.22 as the P-Δ moments vary from a straight line distribution to a sinusoidal distribution.

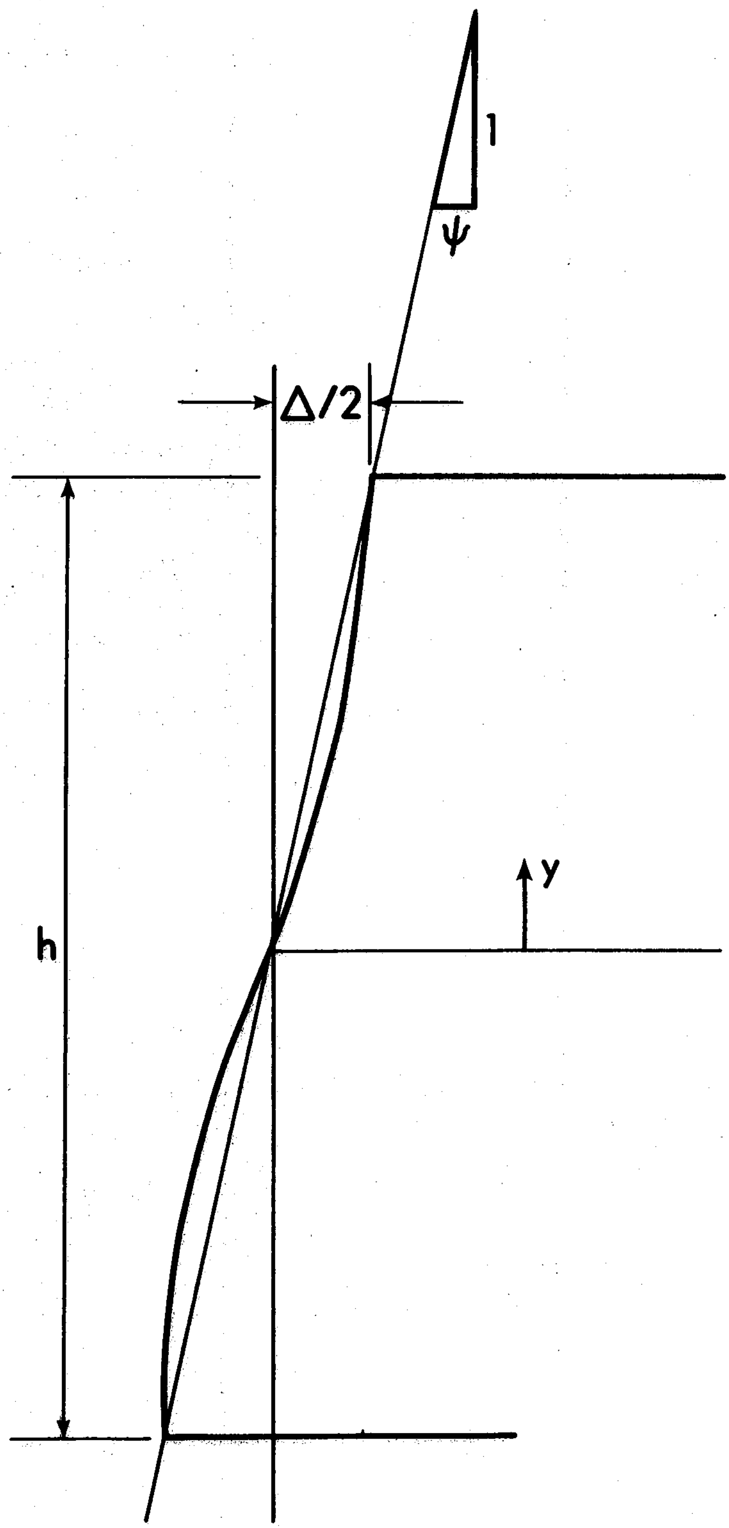

FIGURE 2.2 ISOLATED COLUMN WITH RIGID BEAMS

This is a function of P/P_{cr} and of the relative stiffnesses of the columns and beams.

$$\Delta_2 = \frac{H}{K_\ell - \frac{\alpha \Sigma P}{h}} \qquad 2.8$$

$$M_2 = hH \left[1 + \frac{\frac{\Sigma P}{h}}{K_\ell - \frac{\alpha \Sigma P}{h}} \right] \qquad 2.9$$

The tilting effect of foundation rotation and of column shortening and lengthening in an unsymmetrical building may be taken into account by including these terms in Δ_1.

2.2.2 Frame Buckling

The sway buckling load of a storey can be obtained by solving Equations 2.8 and 2.9 with H set equal to zero.

For a non-trivial solution $\alpha \Sigma P/h$ must equal K_ℓ in Equation 2.8. Therefore, the critical load for the storey under consideration is

$$\Sigma P_{cr} = \frac{K_\ell h}{\alpha} \qquad 2.10$$

since $K_\ell = H/\Delta_1$ this may be rewritten as:

$$\Sigma P_{cr} = \frac{Hh}{\Delta_1} \qquad 2.11$$

where α has been taken equal to 1.0.

2.3 Review of Second-Order Analyses

2.3.1 P-Δ Iteration

In section 2.2.1 it was shown that the total storey moment for the frame shown in Fig. 2.1(a) was given by Equation 2.1. The term "P-Δ effect" refers to the extra bending moments which are developed throughout the structure when the vertical forces, ΣP, are displaced laterally through a deflection Δ. These extra moments are not determined by a conventional first-order structural analysis, since such analyses formulate equilibrium on the undeformed structure. If, however, the shear in the storey was artificially increased by an amount $\Sigma P\Delta_2/h$, the sum of the column end moments in the storey as computed by a first-order analysis would be correct.

These principles may be readily extended to a more complex structure. Initially the structure is analyzed under the given loading to obtain the first-order lateral deflections, denoted as Δ_i, Δ_{i+1}, etc. in Figure 2.3. The artificial storey shears, which would produce column end moments equivalent to those caused by the vertical loads, are then computed:

$$V'_i = \frac{\Sigma P_i}{h_i} (\Delta_{i+1} - \Delta_i) \qquad 2.12$$

The storey shears computed by Equation 2.12 may be represented by additional sway forces H' which will produce moments and forces throughout the structure which will simulate the P-Δ effect. The artificial sway forces due to the vertical loads, H'_i, are then computed as the difference between the additional storey shears at each level:

$$H'_i = V'_{i-1} - V'_i \qquad 2.13$$

The sway forces, H'_i, are added to the applied lateral loads, and the structure re-analyzed. When the Δ_i values at the end of a cycle are nearly equal to those of the previous cycle, the method has converged, and the resulting forces and moments now include the P-Δ effect. It should be noted that the sway forces can be either positive or negative.

The application of P-Δ analyses is discussed by Adams[1], Wood, Beaulieu and Adams[12], MacGregor[11] and many others. An example of the application of such an analysis to a tall steel building is given by Springfield and Adams[13].

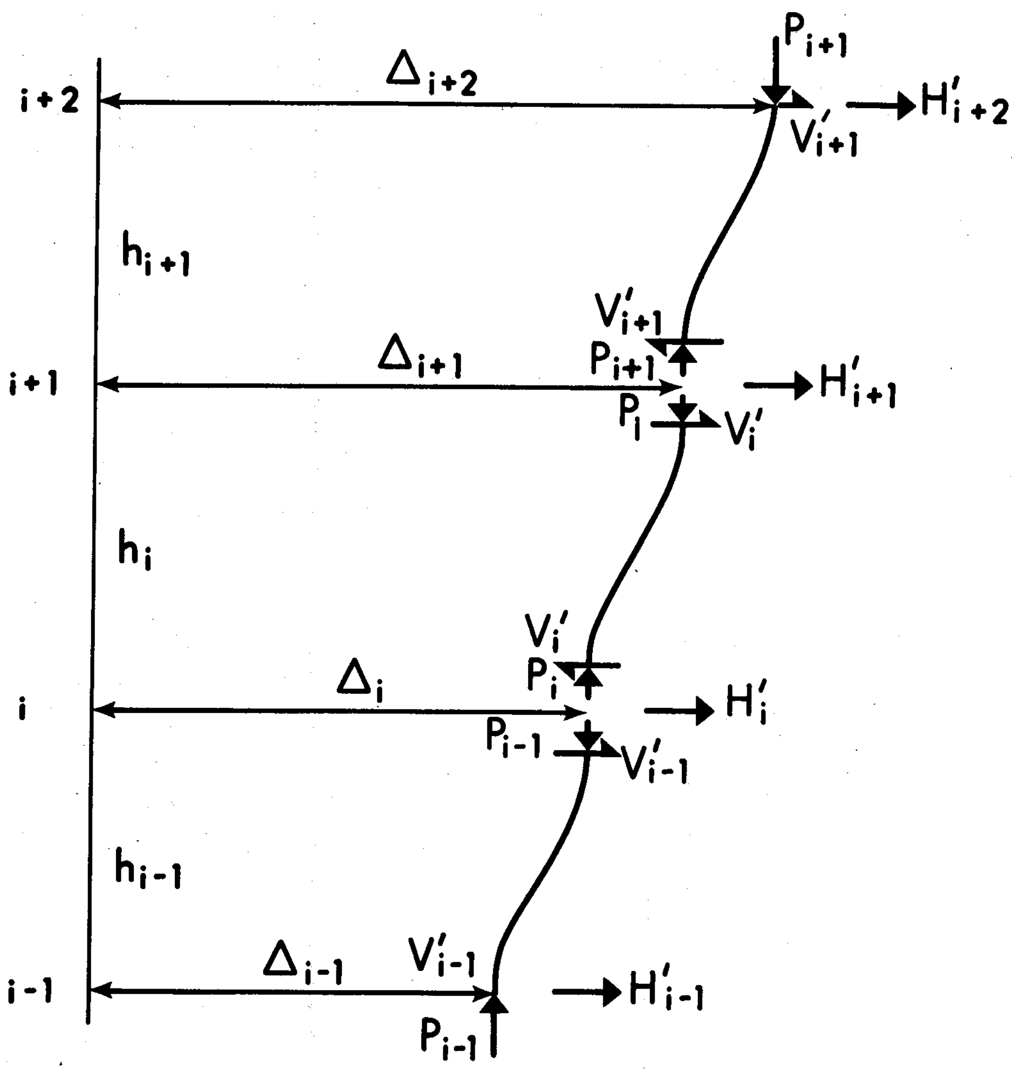

FIGURE 2.3 SWAY FORCES DUE TO VERTICAL LOADS

2.3.2 Simplified Second-Order Frame Analysis

Reference 3 shows that a direct solution of the second-order deflections and moments can be obtained using a standard first-order program by inserting a fictitious diagonal brace of negative area in each storey as shown by the dashed lines in Fig. 2.4(a). The brace area may be obtained by developing the second-order stiffness matrix for the deformed column of Fig. 2.5. Static equilibrium of the column gives:

$$F_t = -\frac{M_t + M_b}{L} - \frac{P(\Delta_t - \Delta_b)}{L} = -F_b \qquad 2.14$$

Substituting the slope deflection equations for M_t and M_b into Equation 2.14 yields the matrix of stiffness influence coefficients given in Equation 2.15.

$$\begin{Bmatrix} M_t \\ M_b \\ F_t \\ F_b \end{Bmatrix} = \begin{bmatrix} 4EI/L & 2EI/L & -6EI/L^2 & 6EI/L^2 \\ 2EI/L & 4EI/L & -6EI/L^2 & 6EI/L^2 \\ -6EI/L^2 & -6EI/L^2 & 12EI/L^3 - P/L & -12EI/L^3 + P/L \\ 6EI/L^2 & 6EI/L^2 & -12EI/L^3 + P/L & 12EI/L^3 - P/L \end{bmatrix} \begin{Bmatrix} \theta_t \\ \theta_b \\ \Delta_t \\ \Delta_b \end{Bmatrix} \qquad 2.15$$

A first-order analysis omits the terms involving P/L. However, if the structure contained bracing members as shown in Fig. 2.4(a), the program would generate a stiffness matrix corresponding to the degrees of freedom shown in Fig. 2.4(b), that is:

$$\begin{Bmatrix} F_t \\ F_b \end{Bmatrix} = \frac{AE}{L_o} \begin{bmatrix} \cos^2\beta & -\cos^2\beta \\ -\cos^2\beta & \cos^2\beta \end{bmatrix} \begin{Bmatrix} \Delta_t \\ \Delta_b \end{Bmatrix} \qquad 2.16$$

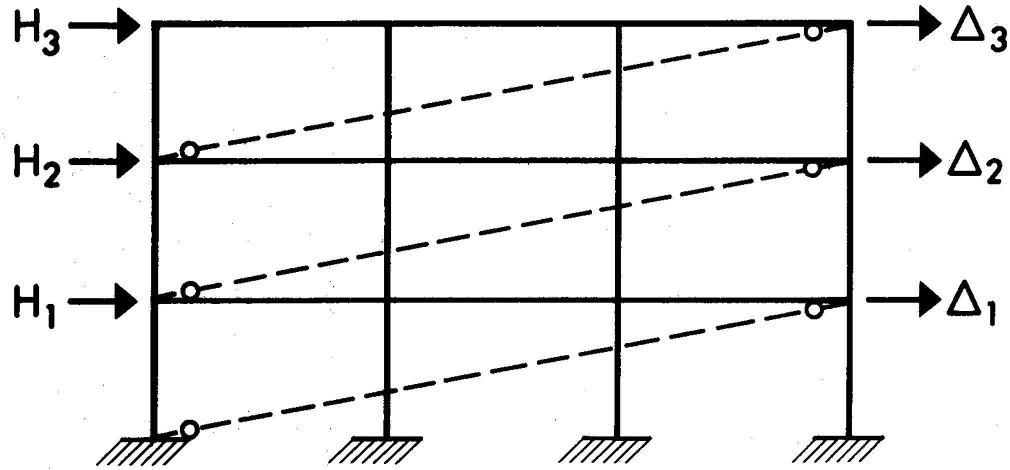

FIGURE 2.4(a) FRAME WITH NEGATIVE BRACING

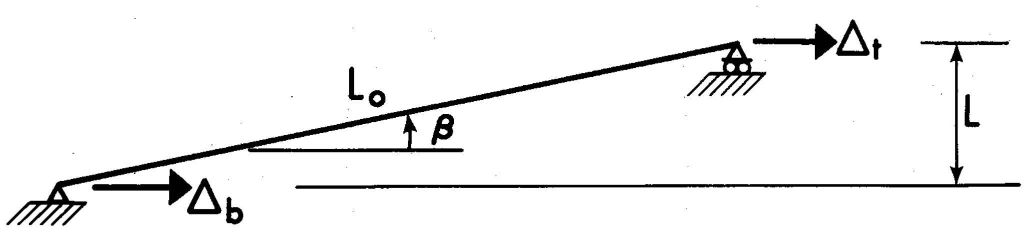

FIGURE 2.4(b) NEGATIVE BRACING MEMBER

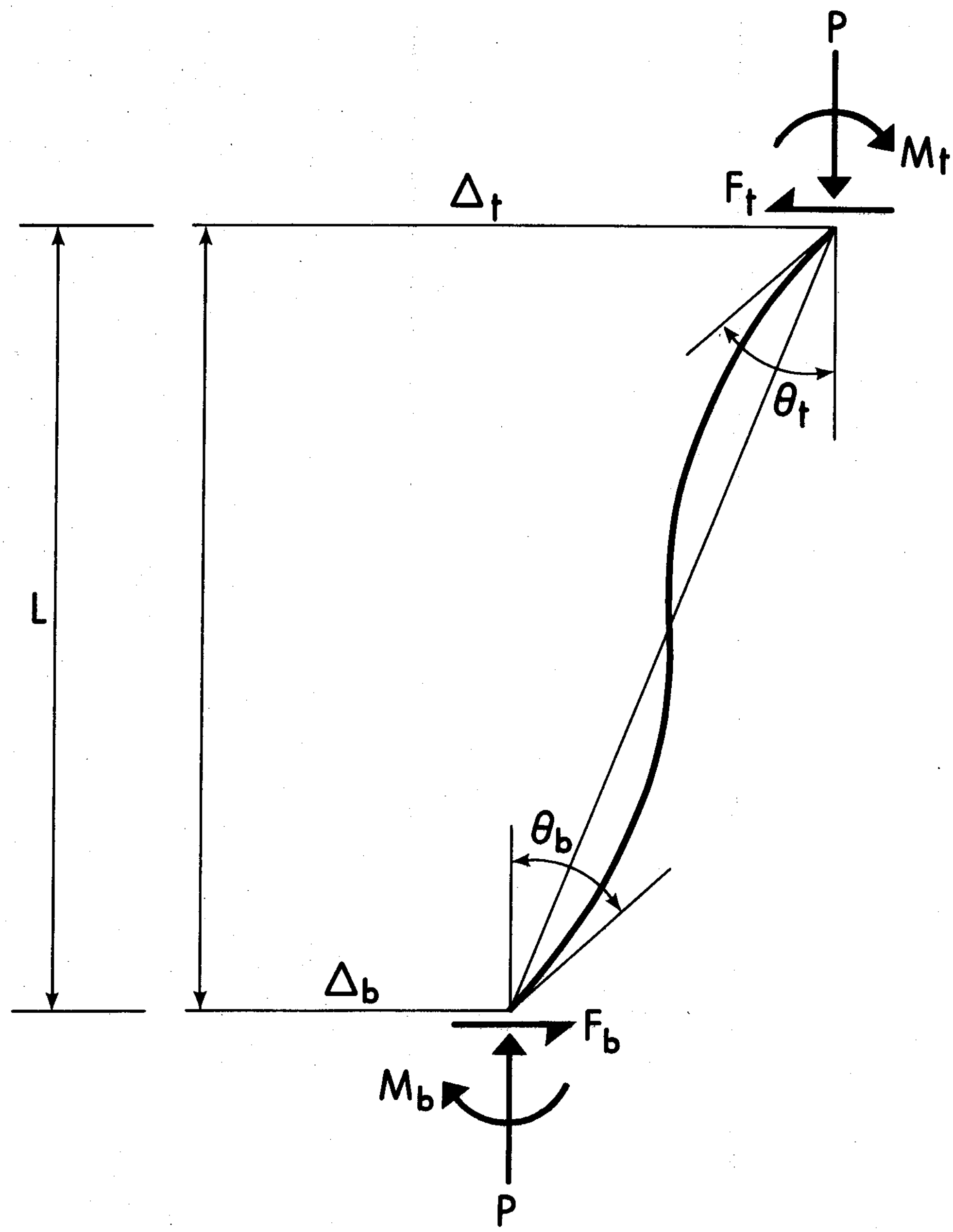

FIGURE 2.5 DEFORMED COLUMN

The two by two matrix would be superimposed in the same position as the P/L terms occupy in the second-order matrix. Considering the brace of the Figure 2.4(b) the required brace area is obtained by equating ($AE/L_o \cos^2\beta$) and ($-P/L$):

$$A = \frac{-P}{L} \frac{L_o}{E\cos^2\beta} \qquad 2.17$$

The value of P in Equation 2.17 represents the sum of the axial loads in the columns of a storey. Because the brace has a negative area, it increases the flexibility of the frame, to account for the P-Δ effect.

A first-order analysis of a structure containing these negative bracing members will compute forces and moments within the structure which correspond to the second-order values. The axial force in the brace causes slight errors in column shears and axial loads which can be corrected by statics. These errors can be kept to a minimum by using long flat bracing members.

2.3.3 Second-Order Finite Element Analysis

K. Aas-Jakobsen(4) has described one type of solution of the second-order moments and forces by means of the finite element method.

If a frame is visualized as an assemblage of elements interconnected at their ends, called nodes, the equilibrium configuration of the complete structure can be expressed in terms of the nodal displacements. The force-displacement relationship for the element of Figure 2.6 can be written as:

$$[K]\ \{w\} = \{P\} \qquad 2.18$$

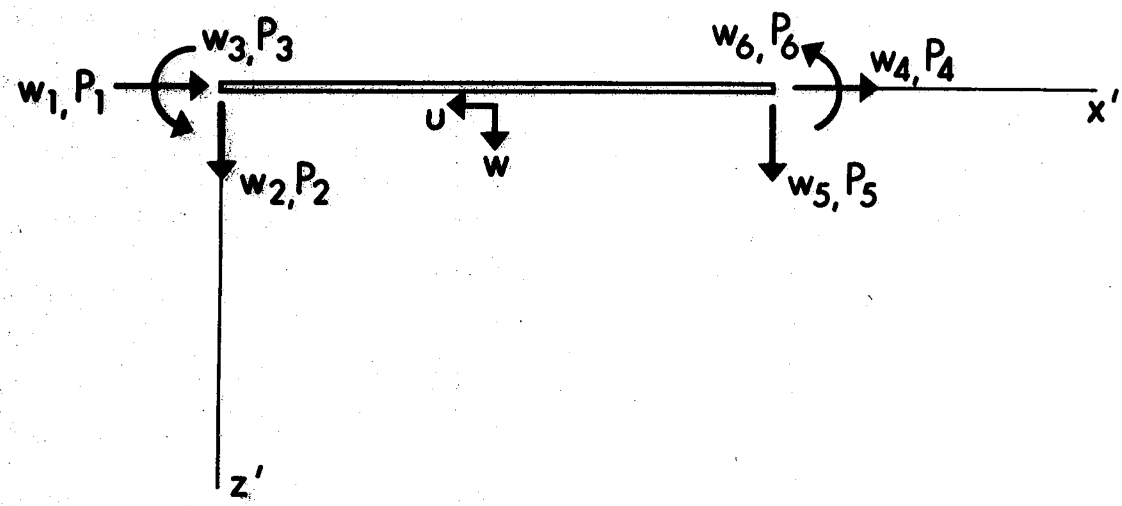

FIGURE 2.6 ELEMENT IN LOCAL COORDINATE SYSTEM

The second-order element stiffness matrix is comprised of two parts, a first-order stiffness matrix, $[K_1]$, and a non-linear geometrical stiffness matrix, $[K_2]$. The matrix $[K_2]$ is unique to the second-order solution and represents the action of axial loads on a deformed element. Both matrices are shown in Figure 2.7.

For an element in a global system, at an angle θ to the local system, the global element stiffness matrix would be given as:

$$[K] = [R]^T [K] [R] \qquad 2.19$$

The element end forces and displacements are transformed as:

$$\{P\} = [R] \{P\}$$

$$\{w\} = [R] \{w\} \qquad 2.20$$

The matrix $[R]$ is shown in Figure 2.8.

The global element stiffness matrix, transformed by Equation 2.19, is shown in Figure 2.9.

Similar to the force-displacement relationship for the element the force-displacement relationship for the complete structure, or the complete system of elements, can be written as:

$$[K] \{w\} = \{P\} \qquad 2.21$$

in which $\{w\}$ now contains all nodal displacements and $\{P\}$ all nodal loads.

Superposition of the individual element stiffness matrices is used to obtain the stiffness matrix for the complete structure.

Restrained displacements, boundary conditions, may be taken into account by greatly magnifying the corresponding diagonal

$$[K_1] = \begin{bmatrix} \frac{EA}{L} & & & \frac{-EA}{L} & & \\ & \frac{12EI}{L^3} & \frac{6EI}{L^2} & & \frac{-12EI}{L^3} & \frac{6EI}{L^2} \\ & & \frac{4EI}{L} & & \frac{-6EI}{L^2} & \frac{2EI}{L} \\ & \text{Symetric} & & \frac{EA}{L} & & \\ & & & & \frac{12EI}{L^3} & \frac{-6EI}{L^2} \\ & & & & & \frac{4EI}{L} \end{bmatrix} \qquad [K_2] = P_x \begin{bmatrix} & & & & & \\ & \frac{6}{5L} & \frac{1}{10} & & \frac{-6}{5L} & \frac{1}{10} \\ & & \frac{2L}{15} & & \frac{-1}{10} & \frac{-L}{30} \\ & \text{Symetric} & & & & \\ & & & & \frac{6}{5L} & \frac{-1}{10} \\ & & & & & \frac{2L}{15} \end{bmatrix}$$

Fig. 2.7 First-Order and Geometric Stiffness Matrices

$$[R] = \begin{bmatrix} c & s & & & & \\ -s & c & & & & \\ & & 1 & & & \\ & & & c & s & \\ & & & -s & c & \\ & & & & & 1 \end{bmatrix} \qquad \begin{matrix} s = \sin\theta \\ c = \cos\theta \end{matrix}$$

Fig. 2.8 Transformation Matrix [R]

$$[K_1] = \begin{bmatrix} \frac{EA}{L}c^2 + \frac{12EI}{L^3}s^2 & (\frac{EA}{L} - \frac{12EI}{L^3})sc & \frac{-6EI}{L^2}s & -k_{11} & -k_{12} & k_{13} \\ & \frac{EA}{L}s^2 + \frac{12EI}{L^3}c^2 & \frac{6EI}{L^2}c & -k_{12} & -k_{22} & k_{23} \\ & & \frac{4EI}{L} & -k_{13} & -k_{23} & \frac{2EI}{L} \\ & & & k_{11} & k_{12} & -k_{13} \\ & \text{Symmetric} & & & k_{22} & -k_{23} \\ & & & & & k_{33} \end{bmatrix}$$

$c = \cos\theta$

$s = \sin\theta$

$$[K_2] = P \times \begin{bmatrix} \frac{6}{5L}s^2 & \frac{-6}{5L}sc & \frac{-1}{10}s & -k_{11} & -k_{12} & k_{13} \\ & \frac{6}{5L}c^2 & \frac{1}{10}c & -k_{12} & -k_{22} & k_{23} \\ & & \frac{2L}{15} & -k_{13} & -k_{23} & \frac{-L}{30} \\ & \text{Symmetric} & & k_{11} & k_{12} & -k_{13} \\ & & & & k_{22} & -k_{23} \\ & & & & & k_{33} \end{bmatrix}$$

Fig. 2.9 Global Element Stiffness Matrix $[K] = [K_1] + [K_2]$

stiffness influence coefficient. A number in the order of 10^{50} was suggested by Aas-Jakobsen.

The axial force P must be known in order to evaluate the element matrix $[K_2]$ in Fig. 2.9. The axial force is usually not known in advance, and an iterative procedure must be used. In the first cycle P is chosen equal to zero and the first order forces are calculated. In the second cycle the axial forces found in the first cycle are used.

Usually the axial forces are practically not influenced by the second-order effects, such that two cycles are generally sufficient.

In checking the accuracy of the method it was found that the calculated moments for frames permitted to sway were in excellent agreement with the exact ones when the columns were represented by one element. For braced columns and frames the errors in moments were as large as 10 percent when the columns were represented by one element but vanished when the columns were divided into two elements.

CHAPTER 3

SELECTION AND SECOND-ORDER ANALYSIS OF BUILDINGS

3.1 Introduction

In this chapter eleven building frames are derived. The characteristics and loading conditions of each frame are discussed. Also, the "exact" method of second-order analysis used to check the approximate results is presented.

3.2 General Information

3.2.1 Material Characteristics

All frames studied were assumed to be constructed of normal weight concrete with a strength of 4000 psi. The elastic modulus of the concrete was given by the ACI Code[7] expression, Equation 3.1:

$$E_c = 57{,}000\sqrt{f'_c} \qquad 3.1$$

The moment of inertia for all members was based on the overall dimensions of the section. To represent the effect of cracking at ultimate conditions the moment of inertia of the columns and beams was multiplied by 0.8 and 0.4, respectively. These values were arbitrarily selected based on studies by Hage[9] and the values proposed by Kordina[14]. The moments of inertia of the shear walls at ultimate were multiplied by 0.4 over their entire height, which, in effect, corresponds to the assumption that the wall is cracked over its entire height.

At service loads the members were assumed to be uncracked and the gross moment of inertia was used.

Creep deformations were not considered since the lateral loads were all of short duration.

3.2.2 Loading Conditions

All buildings were analyzed under combined dead and live load. The dead load values were taken as:

i) Frame self-weight.

ii) Superimposed dead load, including weight of slabs, mechanical equipment and roofing weighing 80 psf on the roof and 100 psf on the floors.

iii) Exterior walls weighing 50 psf of surface area.

The live load values were taken as:

i) Rectangular wind distribution of 20 psf.

ii) Superimposed live load of 30 psf on the roof and 100 psf on the floors.

The frames were analyzed at service and ultimate conditions. The loading cases were:

Service: $1.0(D + L + W)$

Ultimate: $0.75(1.4D + 1.7L + 1.7W)$

where the load combination factor, 0.75, and the load factors, 1.4 and 1.7, for the ultimate load case are those of the 1971 ACI Building Code and CSA A23.3-1973.

Wind loading was applied as a concentrated load at each floor level applied along the left column line. The right column line is therefore denoted as the leeward face. Exterior walls, as noted, also formed a dead load component. This loading was lumped into a point load applied vertically at each floor level.

3.3 Details of Frames Studied

Figures 3.1 to 3.5 present the geometry and member sizes of the frames studied. Frames one to five and eight to eleven are assumed to be typical interior frames in buildings containing no bracing not already included in the typical frames. In all cases the transverse spacing of the frames in the building is assumed to be twenty feet, which means the wind pressure, dead and live loads act over a twenty foot tributary width.

Frame type one is a twenty storey, two bay structure as shown in Figure 3.1. The sizes of the beam and column cross-sections are given immediately to the right of the frame elevation and apply to all frames in that figure. The larger of the two column sizes given denotes the size of the interior column. The smaller dimensions refer to both exterior columns.

With frame type one it was desired to represent a fairly regular structure with a uniform change in stiffness along its height.

Frame type two, also shown in Figure 3.1, is essentially the same as type one. It was desired, however, to investigate the effect of a tall and more flexible ground storey, hence the first storey was enlarged from twelve to eighteen feet.

Figure 3.2 illustrates frame type three which was chosen to represent a structure of essentially constant stiffness. One change in column sizing was introduced at mid-height of the building because it was desired to investigate the effect of the uniform stiffness yet represent a feasible structure.

Frame types four and five are shown in Figure 3.3. Both represent shear wall frames with exterior columns and beams the same as those of frame type one. The size of the shear wall in type four was assumed to be such that its moment of inertia was five times the sum of the moments of inertia of the exterior columns. For purposes of analysis the wall was input into the program as a straight line member ignoring the effect of the wall width. Also, as previously mentioned in section 3.2.1, the moment of inertia of the shear wall at ultimate was taken as 0.4 times the gross moment of inertia over the total height of the wall. Since some of the wall would probably not crack in all storeys, the effect of wall cracking is probably overestimated.

Frame type five was chosen to investigate the effect of a heavier wall than that found in type four. In this stiffer structure the wall moment of inertia at service loads was taken as fifty times the sum of the moments of inertia of the exterior columns.

Figure 3.4 shows the plan of buildings six and seven. The plan shown is one half of a symmetrical structure. The building is a flat plate structure with dimensions as shown. The slab thickness is taken as seven and one half inches at every floor level. Column and shear wall sizing is constant for the total height of the building.

In modelling this twenty storey building, the frames were lumped together and linked to the shear wall-frame as shown in Figure 3.5. The six inch links were pinned at each end and made axially stiff to represent a rigid floor diaphragm. The shear wall was modelled as a vertical member with the correct axial stiffness along the center-line of the wall and with essentially rigid arms extending from the wall centerline to the ends of the floor beams in each floor. This allowed the use of a common plane frame analysis program.

Frame type six is shown in elevation in Figure 3.5. Frame type seven was essentially the same as type six only that the shear wall was terminated at the seventeenth storey and replaced by two lines of columns above this level. This was done to investigate a frame subjected to the whipping action which might develop due to the change in stiffness.

Frame types eight to eleven, shown in Figure 3.1, represent a series of special case structures. These four frames are based upon the geometry and member sizes of frame type two incorporating various modifications to introduce soft storeys.

Frame type eight was created from type two by deleting the second floor, thus creating a thirty foot first storey. Frame type nine was formed by deleting the tenth storey of type two. Frame type ten was the most radical frame analyzed and was created by deleting the second, tenth and top floors of type two. In each of these three buildings it was desired to study the effect of the discontinuities. It should be noted that these buildings were highly artificial since no attempt was made to stiffen the structure in the vicinity of the missing floors.

Frame type eleven was identical to type two in construction. However, increased loads, were applied to the roof and top two floors. The roof and floors of the nineteenth and twentieth storeys were subjected to a superimposed dead load of 480 psf and 500 psf, respectively. This additional load served to represent mechanical floors, and tended to increase the P-Δ effect.

3.4 "Exact" Second-Order Analysis

To provide a check on the approximate methods of analysis it was required to perform an accurate second-order analysis on each frame. The negative bracing member method, as discussed in section 2.3.2, was used to do this. A negative brace was sized for each storey and inserted with positive slope extending from the bottom of the windward exterior column to the top of the leeward exterior column.

The analyses were carried out using the program PFT (plane frames and trusses) described by Beaufait et al[15].

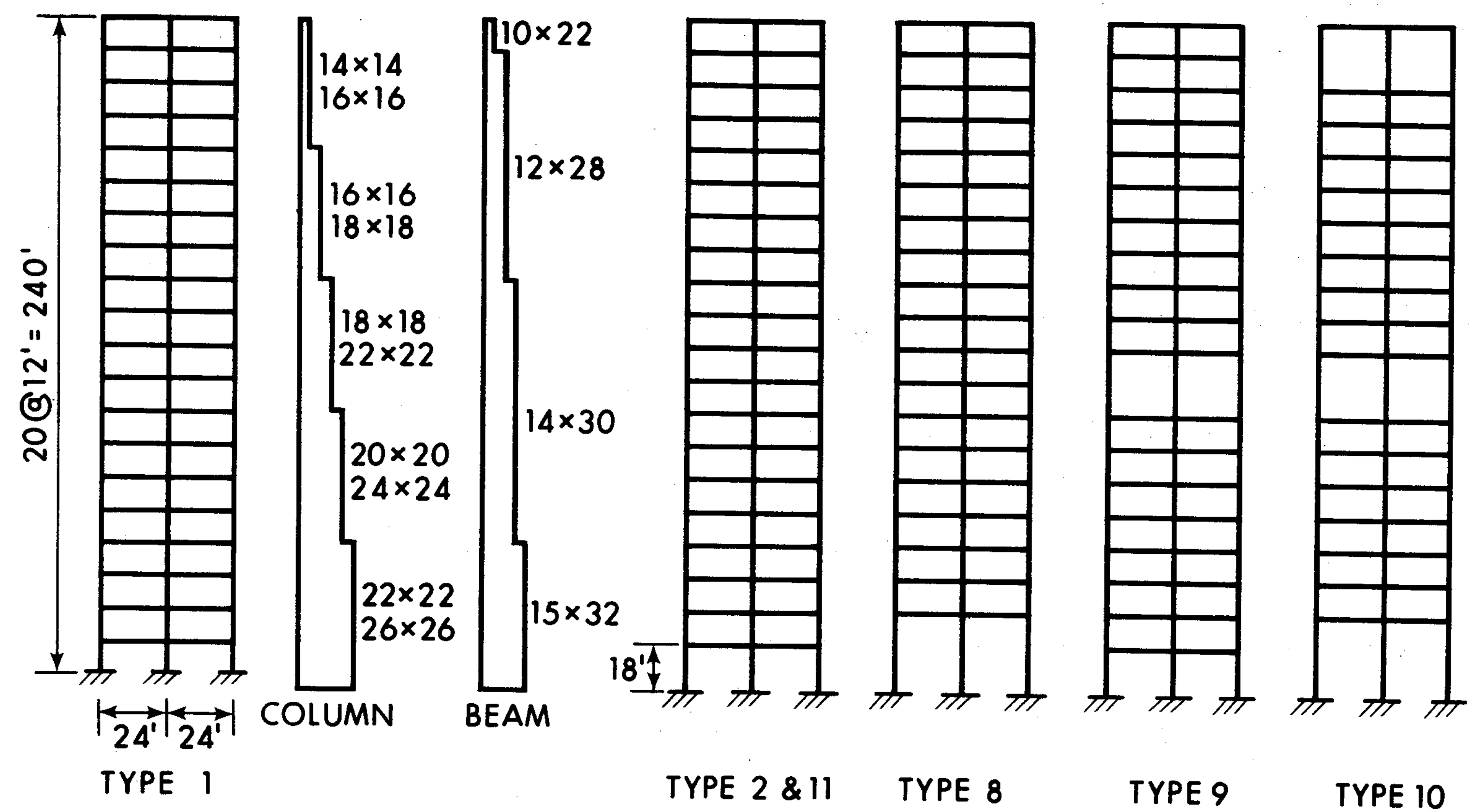

FIGURE 3.1 FRAME ELEVATIONS

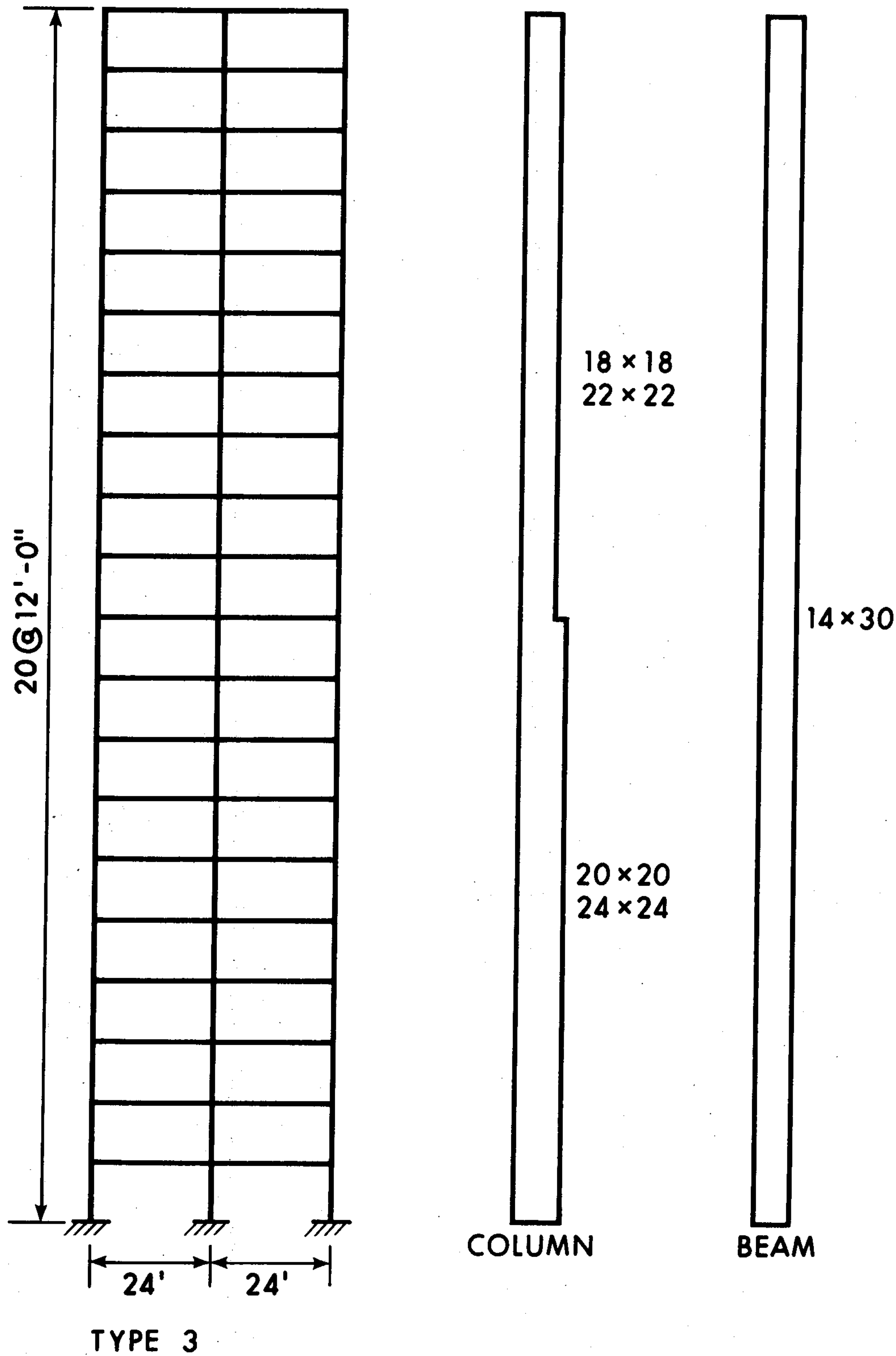

FIGURE 3.2 ELEVATION OF FRAME TYPE THREE

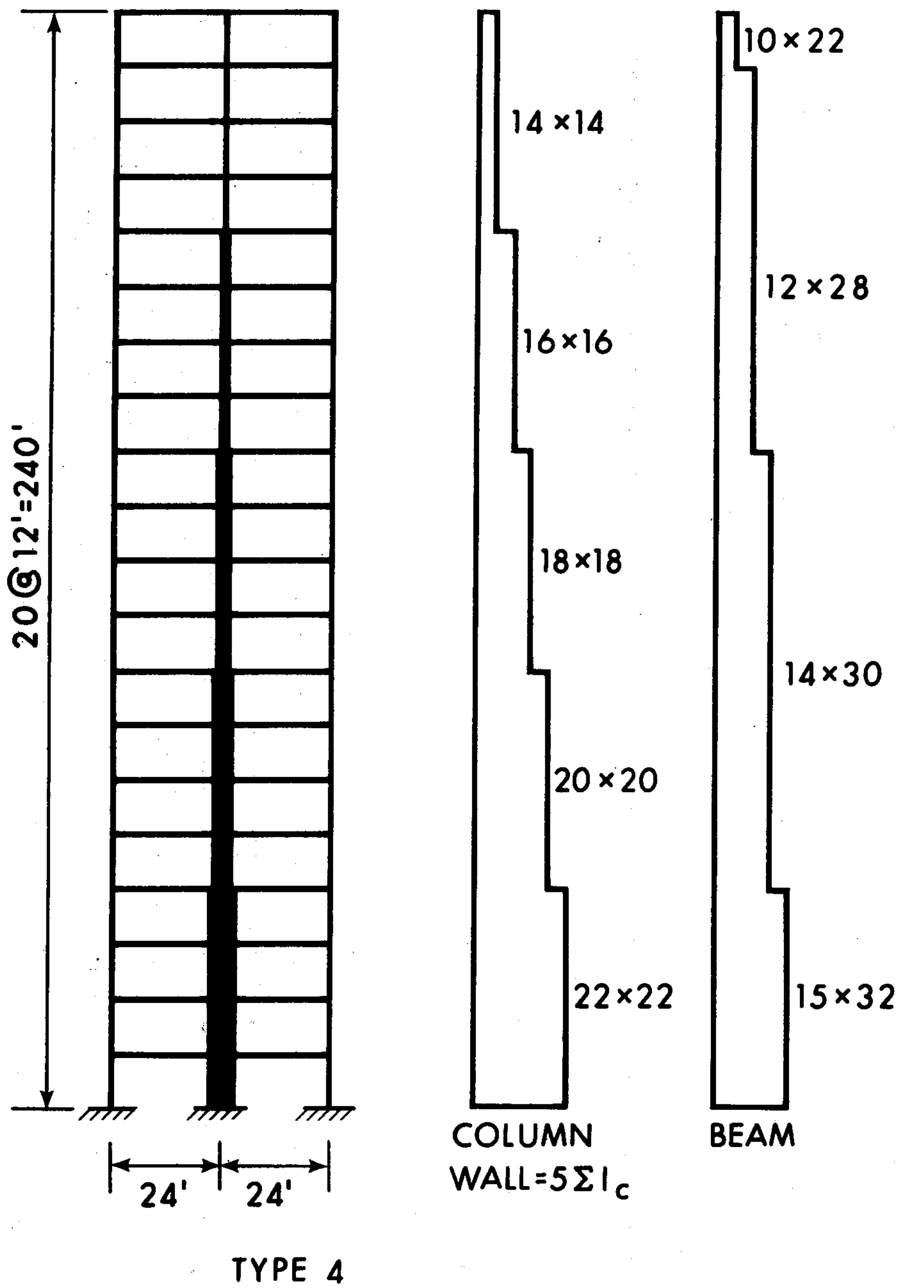

(Type 5 similar with wall = 50 ΣI_c)

FIGURE 3.3 ELEVATION OF FRAME TYPE FOUR

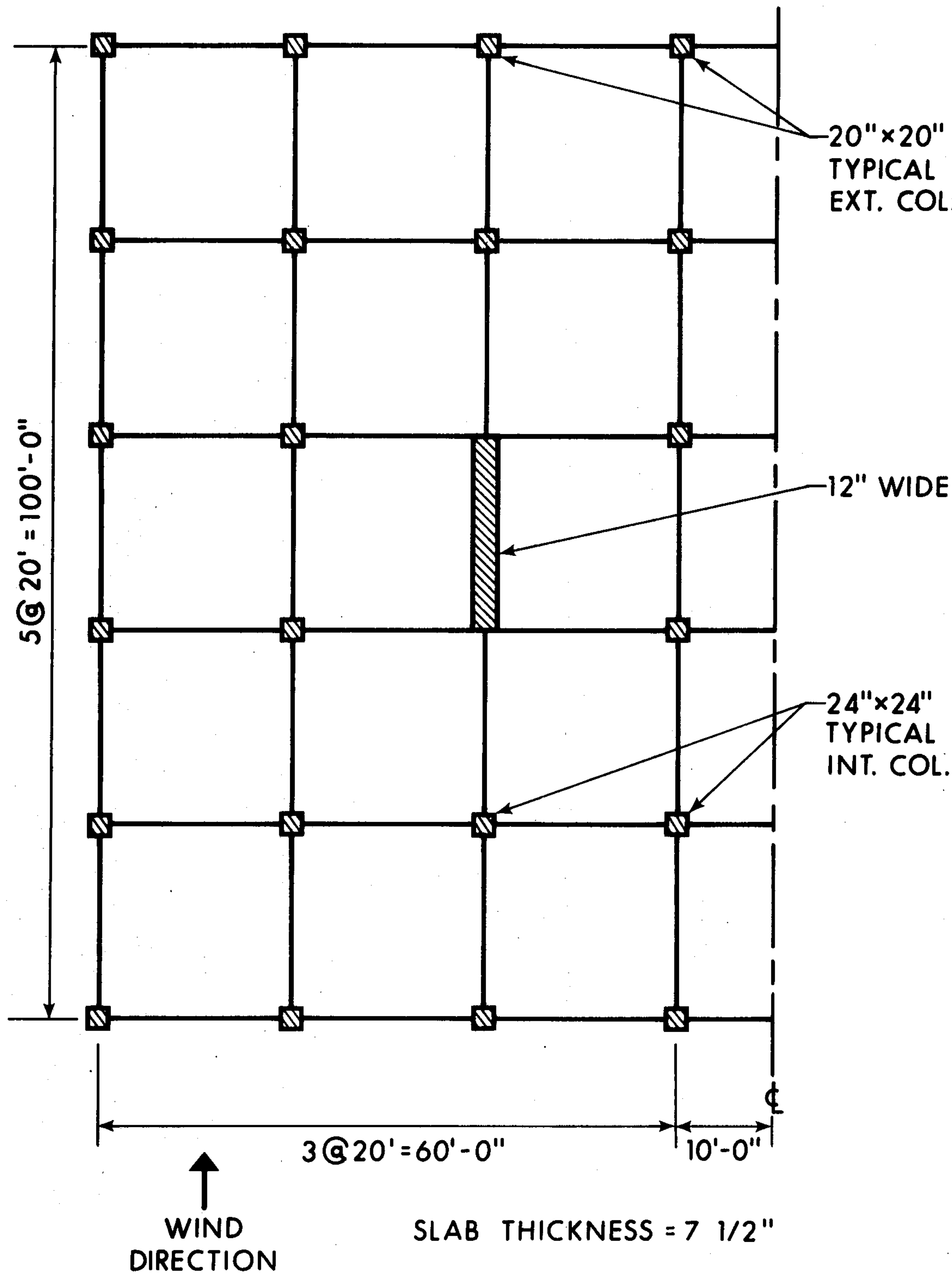

FIGURE 3.4 PLAN OF FRAME TYPE SIX

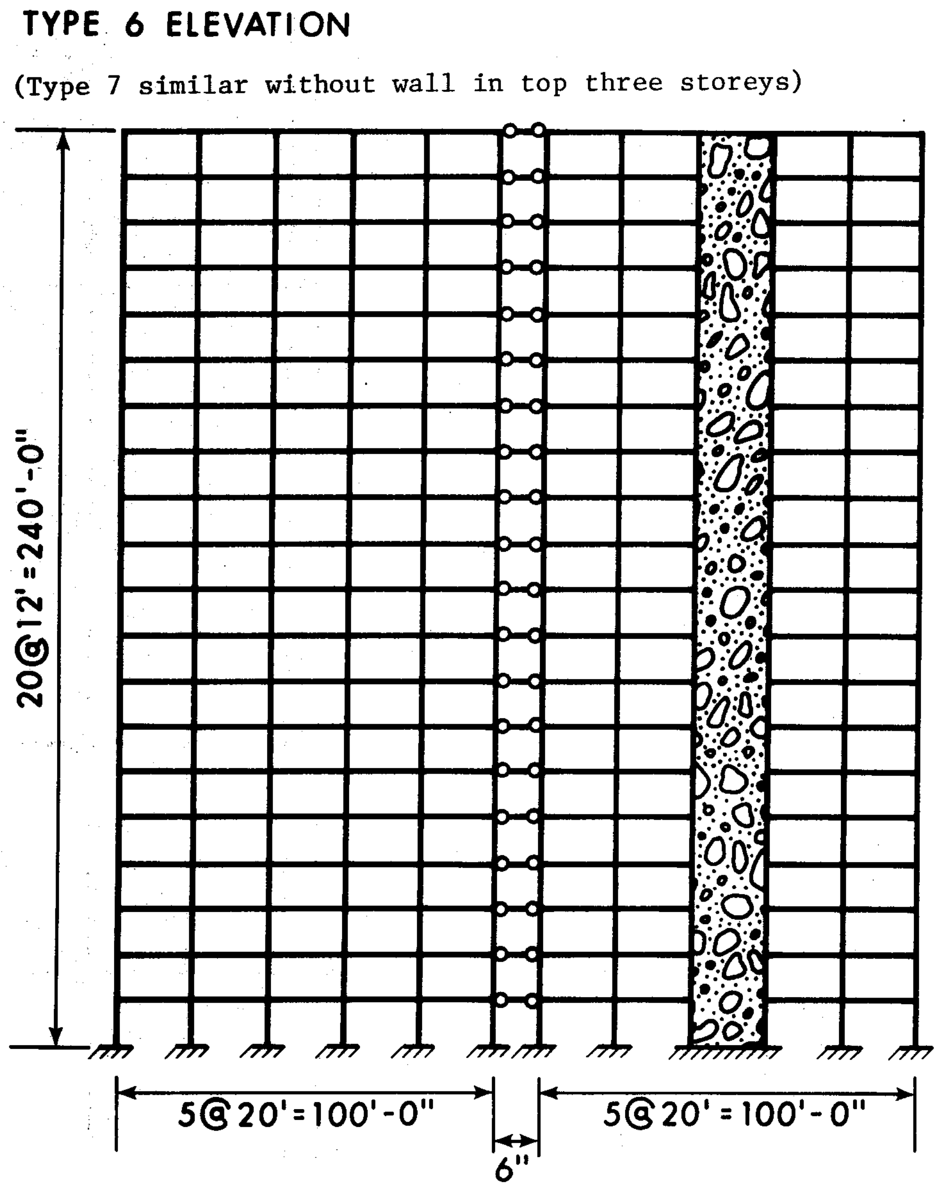

FIGURE 3.5 ELEVATION OF FRAME TYPE SIX

CHAPTER 4

APPROXIMATE ANALYSIS

4.1 Introduction

Section 4.2 of this chapter presents the theory behind three approximate methods of second-order analysis which will be compared to accurate P-Δ analyses. These are the Fey method, the moment magnifier method and the amplified lateral load method. The procedure used to apply each method to the frames described in Chapter three is also discussed. The errors associated with each method are presented in graphical form and is discussed in section 4.3.

The column moments obtained by each analytical procedure are summarized in figures presented in Appendix A.

4.2 Theory and Application of Analyses

4.2.1 Fey Method

From the theory of section 2.2 it is seen that the second-order deflections may be estimated from the first-order deflections by the equation:

$$\Delta_2 = \frac{\Delta_1}{1 - \frac{\Sigma P \Delta_1}{Hh}} \qquad 4.1$$

where,

ΣP = total vertical load on the storey.

H = total lateral shear on the storey.

This equation was derived by Fey[17], Goldberg[18] and in a slightly different form by Parme[19]. Equation 4.1 was used to estimate second-order moments in the manner described in the rest of this paragraph. Initially, a first-order analysis was conducted on each frame at ultimate conditions. The relative lateral floor displacements then gave the Δ_1 value for each storey. Knowing the values of ΣP, H, and the storey height, h, the value of Δ_2 was calculated for each storey from Equation 4.1. The Δ_2 values for each storey then gave a displaced structure which approximated the final shape including the second-order effects. Based on these final approximate deflections, column end shears were determined as outlined in section 2.3.1. Using these end shears, sway forces equal to the difference in end shears taken with the appropriate sign were calculated. Finally, these sway forces were added to the original lateral load, and the total lateral loads were used to estimate the second-order forces, moments and deflections. Both the lateral and vertical load moments can be obtained together in this analysis if desired.

Use of the Fey equation (Eqn. 4.1) avoided the necessity for several cycles of iteration to compute Δ_2 and the second-order moments and forces.

The analysis described above was carried out at the ultimate load level. The results from this analysis will be compared to an "accurate" second-order analysis in section 4.3.

4.2.2 Moment Magnifier Method

Considering the column of Figure 4.1, the bending moment, M_2, at the base of the column shown by the dashed lines is:

$$M_2 = Hh + \Sigma P \Delta_2 \qquad 4.2$$

If the critical load for the column is denoted by P_{cr} and $Q = \Sigma P/P_{cr}$ then Δ_2 is given as:

$$\Delta_2 = \left(\frac{1}{1-Q}\right) \Delta_1 \qquad 4.3$$

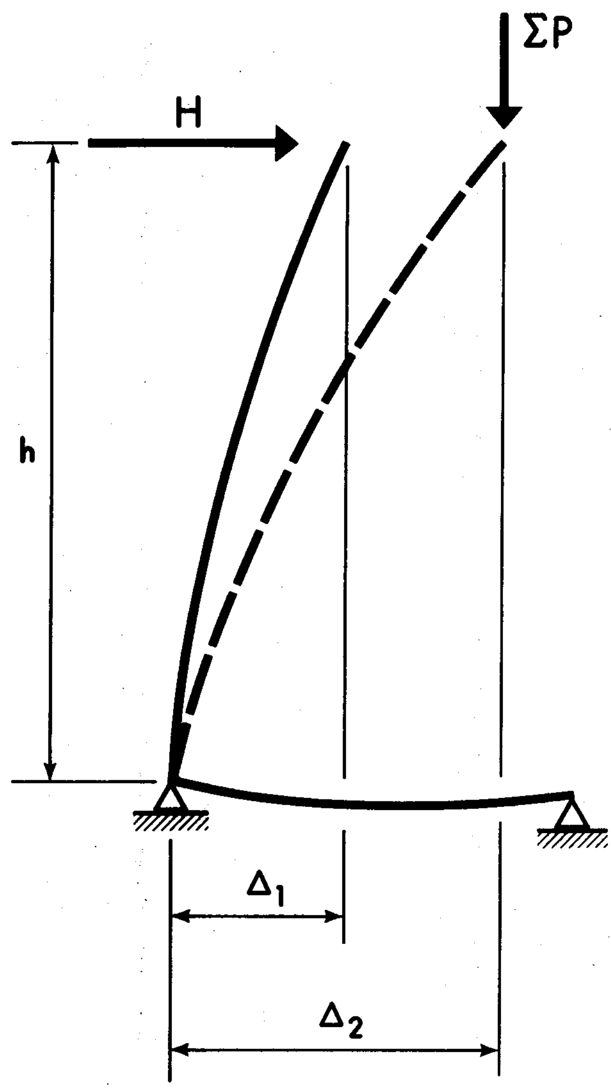

FIGURE 4.1 FORCES ON DEFLECTED COLUMN

and the second-order bending moment is given as:

$$M_2 = Hh + \Sigma P\Delta_1 \left(\frac{1}{1-Q}\right) \qquad 4.4$$

From the theory of section 2.2 the value of Q may be approximated by:

$$Q = \frac{\Sigma P\Delta_1}{Hh} \qquad 4.5$$

and the second-order moment, M_2, can be approximated by:

$$M_2 = Hh + Hh \left(\frac{Q}{1-Q}\right) = Hh \left(\frac{1}{1-Q}\right) \qquad 4.6$$

Thus, for a given lateral loading pattern leading to first-order frame moments, M_1, the total second-order moment, M_2, is given as:

$$M_2 = M_1 \delta \qquad 4.7$$

where

$$\delta = \frac{1}{1-Q} = \frac{1}{1 - \frac{\Sigma P\Delta_1}{Hh}} \qquad 4.8$$

Initially, two first-order analyses were conducted on each frame at ultimate conditions, one with vertical frame loading only, the second with lateral loading only. From the first-order lateral load analysis a value of Q, as given by Equation 4.5, was determined for each storey. The moment magnifier, δ, for each storey was then computed by Equation 4.8. The column end moments obtained from the first-order lateral load analysis were then magnified. These magnified moments were added to those from the vertical load analysis to obtain final end moments.

4.2.3 Amplified Lateral Load Method

This method attempts to amplify the lateral load such that convergence upon the final second-order moments is obtained in one analysis. The lateral loads to be used in the analysis are taken as $1/(1-Q_u)$ times the actual lateral loads where $Q_u = (\Sigma P_u/H_u)(\Delta_u/h)$. Initially, Q_u is based on an assumed drift (Δ_u/h). If the value of Δ_u/h in any storey computed in the frame analysis exceeds the assumed value, the designer would have to rerun the analysis with still larger lateral loads, or preferably, he should revise the structural framing to reduce Δ_u/h to the desired value.

The serviceability reasons it is necessary to know the total (ie. second-order) deflections at service loads. Reference (9) has shown that the EI at service loads is roughly 1.7 times that at ultimate loads. For the wind loading case the ACI load factors are 1.05 Dead + 1.28 Live + 1.28 Wind. Thus, the first-order lateral load deflection at ultimate is 1.28 x 1.7 = 2.2 times the first-order service load deflection. However, from Equation 4.1, the relationship between service load and ultimate load deflections can be estimated as:

$$\frac{\Delta_{2s}}{h} = \frac{\Delta_{1s}/h}{1 - \dfrac{\Sigma P_s \Delta_{1s}}{H_s h}} \qquad 4.9$$

and

$$\frac{\Delta_{2u}}{h} = \frac{\Delta_{1u}/h}{1 - \dfrac{\Sigma P_u \Delta_{1u}}{H_u h}} \qquad 4.10$$

where the subscripts s and u refer to service and ultimate loads respectively. If we let $(\Delta_{2s}/h) = c(\Delta_{2u}/h)$, $H_u = 1.28\ H_s$,

$(\frac{\Delta_{2u}}{h})/(\frac{\Delta_{2s}}{h})$ = K and P_u = (1.05 to 1.28) P_s then from Equations 4.9 and 4.10 we get:

$$c = \frac{1}{K}\left[\frac{1 - Q_u}{1 - \frac{Q_u}{(1.05 \text{ to } 1.28) \times 1.7}}\right] \qquad 4.11$$

For the eleven frames studied the value of K varied from 2.04 to 2.51, with an average value for frame buildings of 2.11 and for buildings with walls of 2.42. The latter value is expected to be on the high side in practice since in the analyses the wall was assumed cracked in all storeys. In applying this method to the eleven frames, the first-order deflection at ultimate was taken as 2.2 times the first-order service load deflection (K = 2.2), which was roughly the average value for all eleven buildings. Establishing Q_u = 0.2, which is a reasonable upper limit on the allowable value of Q for a storey and solving Equation 4.11 for a lower bound, gave c = 0.40. Thus, the ratio between the total second-order drift at service and ultimate conditions is estimated to be 0.40.

In carrying out a design, the designer would determine the service load sway index required for occupant comfort or to prevent non-structural damage, would divide this by 0.4 and get an estimate of Δ_u/h and use this to compute Q_u and the amplified lateral loads for each storey. The value of Q_u is then computed as:

$$Q_u = \frac{\Sigma P_u}{H_u} \frac{\Delta_{2u}}{h} \qquad 4.12$$

From Equation 4.12 a value of Q_u can be determined for each storey. The amplified lateral load can then be computed as:

$$H_{2u} = \frac{H_u}{1 - Q_u} \qquad 4.13$$

In design, only one first-order frame analysis would be needed and would be carried out using this lateral load.

In order to apply this method to the frames considered in this thesis, a somewhat different procedure was used because the frames had not been designed to meet any particular sway index. Rather than arbitrarily assuming a value of Δ_2/h at service loads, the maximum Δ_{2s}/h value in any storey of each building was used directly. The average second-order service load drift was taken as 0.85 of the maximum value based on studies of the drifts in frames one, two, three and four. The ultimate second-order drift used in comparing this procedure to the accurate analyses was then taken as:

$$\frac{\Delta_{2u}}{h} = \frac{1}{c} \times 0.85 \frac{\Delta_{2s}}{h}$$

$$= 2.125 \frac{\Delta_{2s}}{h}$$

4.3 Comparisons of the Three Approximate Methods to the "Accurate" Analysis

4.3.1 Comparison of Moments

The relative error in each of the approximate methods with respect to the negative bracing solution is herein calculated for each frame and presented graphically. The "error function", e, was defined as the difference in a column end moment between the approximate and "exact" value divided by the total storey moment times 100%. That is:

$$e = \frac{M_{approx} - M_{exact}}{\Sigma(M_{top} + M_{bot})} \times 100\% \qquad 4.15$$

The error function is expressed in this way to show the relative importance of the error when compared to the total moment governing the design of the storey.

A different e can be defined for each end of the column. To condense the presentation, only the error in the larger column end moment was computed since this moment would govern the design of the column. The results are presented in Figures 4.2 to 4.12. The errors are presented for the center-line columns in frames one to five and eight to eleven. The windward column moments were not considered as they were relatively low and would not govern the design. The errors in the leeward side column moments were not plotted since, in general, the errors in these moments were found to be about one-half those of the center line columns. In frames six and seven the errors were calculated in the column line immediately to the left of the shear wall. This corresponded approximately to a central column line and allowed investigation of the effect of the shear wall. In Figures 4.2 to 4.12 the errors corresponding to the Fey method are plotted with solid lines, the moment magnifier method with dashed lines and the amplified lateral load method with broken lines. The horizontal scales change in some of the graphs.

As shown by the graphs, the approximate methods appear generally conservative. In all frames the moments from the Fey method and the moment magnifier method were within two percent with few exceptions, while the amplified lateral load method was generally considerably more conservative. The errors would tend to be higher than expected in practice due to the high degree of flexibility in the frames, which resulted in higher than normal values of $Q = \Sigma P\Delta_1/Hh$ and hence higher than normal second-order effects.

The errors in moments were larger and somewhat more erratic in frame type five than in the other frames for two reasons. The comparisons were carried out for the moments in the shear wall which resisted the majority of the moments hence errors in these moments were a larger percentage of the total storey moment. Secondly, there were large discontinuities in the wall stiffness and inaccuracies appeared at each discontinuity.

Frame types six and seven showed good results. The error values were small and generally conservative. The fact that these frames were stiffer than the other frames studied improved the accuracy of the amplified load method.

For the special case structures, types eight to eleven, the Fey method was the most accurate. The moment magnifier method gave similar results but became inaccurate in the area of the discontinuities, in this case the large storeys. The amplified load method was shown to be grossly conservative due to the fact that the calculations were based on a large storey drift which occurred in the high storeys. In a practical structure this error would be expected to be less since the columns and beams in such a storey would be stiffened to reduce the sway.

4.3.2 Comparison of Deflections

Table 4.1 summarizes the roof deflections for each building. As seen in the table, each approximate method generally overestimates the "exact" tip deflection. At the same time, however, the Fey method and the moment magnifier method give a very good approximation for the more regular frames, types one to five, and the frame-shear wall structures, types six and seven. With these two analyses the approximation for the special case buildings, types eight to eleven, is also good, with errors in deflections of generally less than six percent. The amplified lateral load method gives a greater degree of conservatism in estimating the roof deflection, consistent with the column moment approximations. The error in the amplified lateral load method was approximately ten percent for frames one to seven and ranged as high as fifty percent for the special case buildings, types eight to eleven. As pointed out earlier this was due, in part, to the manner in which these frames were derived with one or more high storeys without increasing the stiffness in these regions.

Table 4.2 illustrates the average second-order drift for each building at ultimate conditions. These values are also compared to the maximum drift in any storey for that building at ultimate conditions. In building types one to seven the maximum storey drift ranged from 1.1 to 1.7 times the average and could be taken roughly as one and a half times the average. In buildings eight to eleven the maximum storey drift was about twice the average. In the derivation of the amplified lateral load method in section 4.2.3 this ratio was taken as 1/0.85 = 1.18. As a result the amplified lateral loads tend to be on the high side.

The computed maximum storey sways at ultimate ranged from 1/323 for frame six to a maximum of 1/76 for frame ten. These values, particularly the second value, are higher than would normally be expected in reinforced concrete buildings at ultimate[21]. Since the accuracy of the approximate methods tended to increase as the frames became stiffer, the inaccuracies observed in the comparisons made will tend to be on the high side.

TABLE 4.1 Comparison of Calculated Roof Deflections

Frame Type	Roof Deflections - Inches						
	Service		Ultimate				
	Δ_1	Δ_2	Δ_1	Δ_2	Δ_{Fey}	$\Delta_{Mom't.\ Mag.}$	$\Delta_{Amp\ Load}$
1	4.69	4.94	10.16	11.73	12.36	12.17	12.77
2	5.09	5.37	10.88	12.64	13.33	13.16	13.69
3	4.55	4.80	9.94	11.69	12.35	12.16	12.93
4	3.96	4.12	9.20	10.49	11.04	10.87	11.74
5	3.33	3.45	7.87	8.82	9.33	9.16	9.33
6	2.07	2.27	5.17	6.62	6.73	6.59	7.16
7	2.05	2.26	5.15	6.68	6.82	6.68	7.01
8	6.07	6.72	12.53	15.67	16.48	16.19	25.82
9	5.84	6.35	12.35	15.11	16.00	15.70	22.79
10	7.04	7.95	14.39	18.64	18.95	18.53	26.70
11	5.07	5.48	10.87	13.52	14.77	14.51	16.11

Δ_2 values from negative brace method.

TABLE 4.2 Comparison of Maximum and Average Sway Angles

Frame Type	Δ_{2u}/h Values		
	Average	Max.	Storey
1	.0041	.0056	(6)*
2	.0043	.0057	(6)*
3	.0041	.0069	(3)*
4	.0036	.0051	(6)*
5	.0031	.0042	(7)*
6	.0023	.0031	(7)*
7	.0023	.0033	(9)*
8	.0053	.0124	(1)*
9	.0051	.0122	(9)*
10	.0063	.0132	(1)*
11	.0046	.0060	(6)*

*Indicates storey in which maximum value occurred.

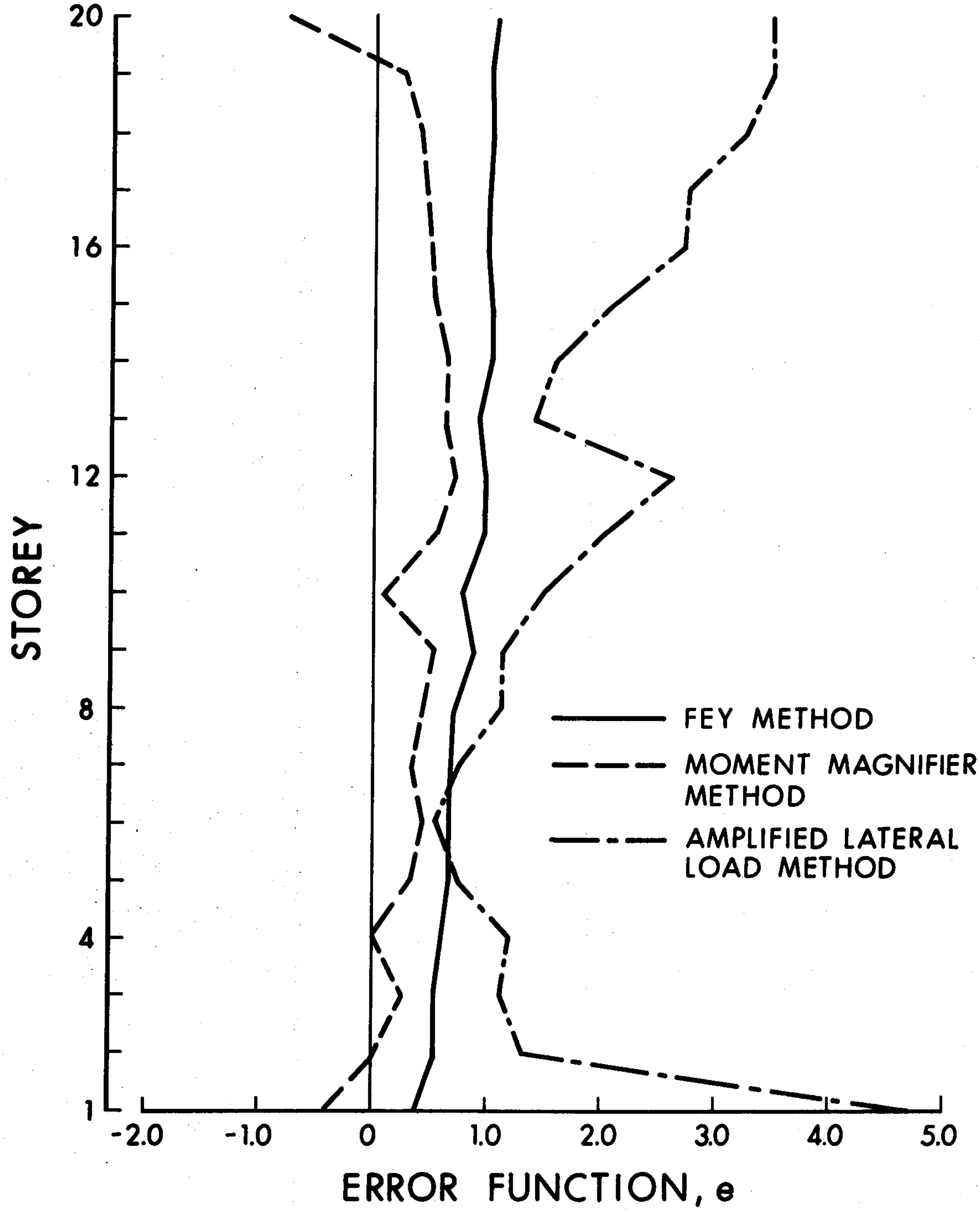

FIGURE 4.2 MOMENT ERRORS IN FRAME TYPE ONE

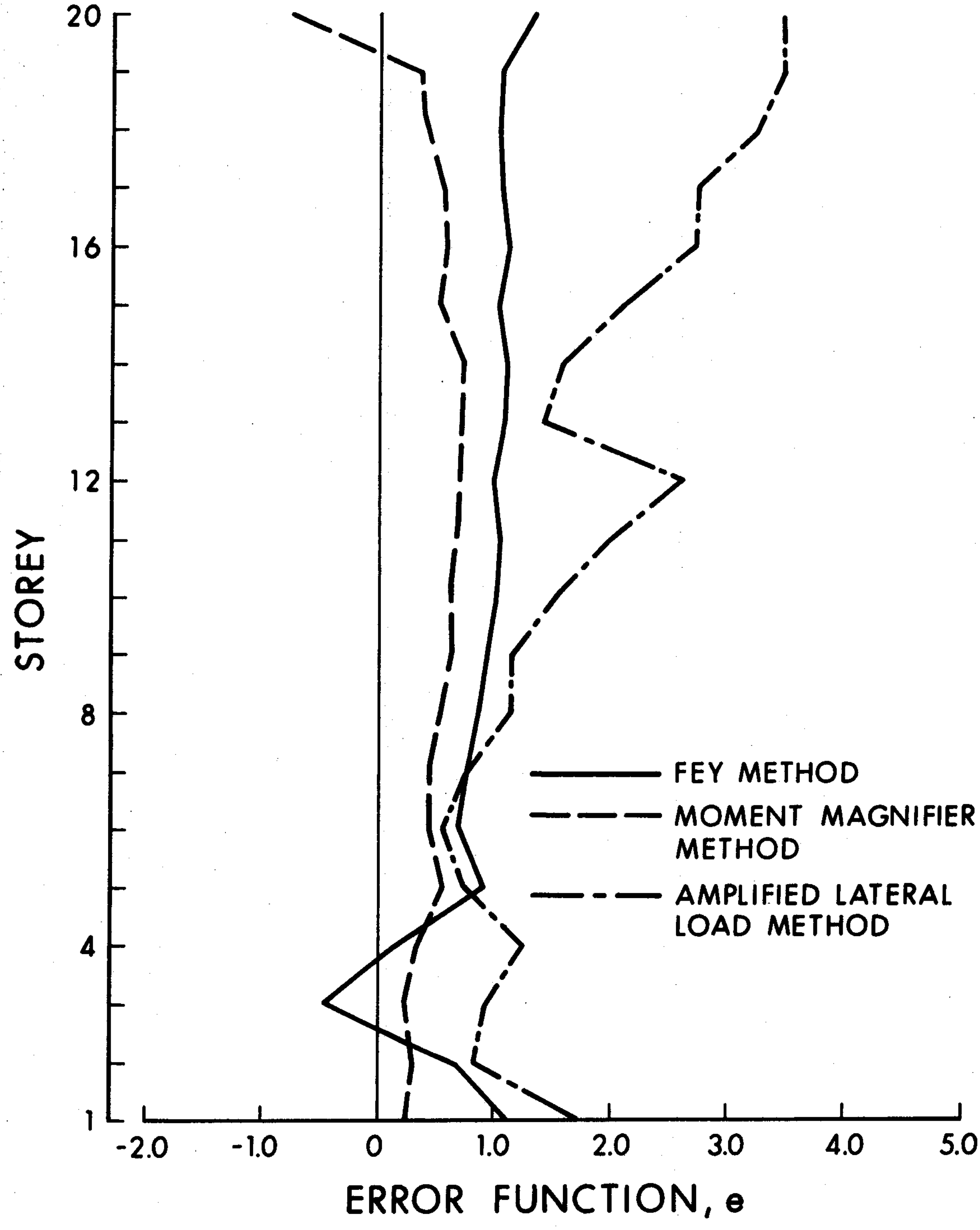

FIGURE 4.3 MOMENT ERRORS IN FRAME TYPE TWO

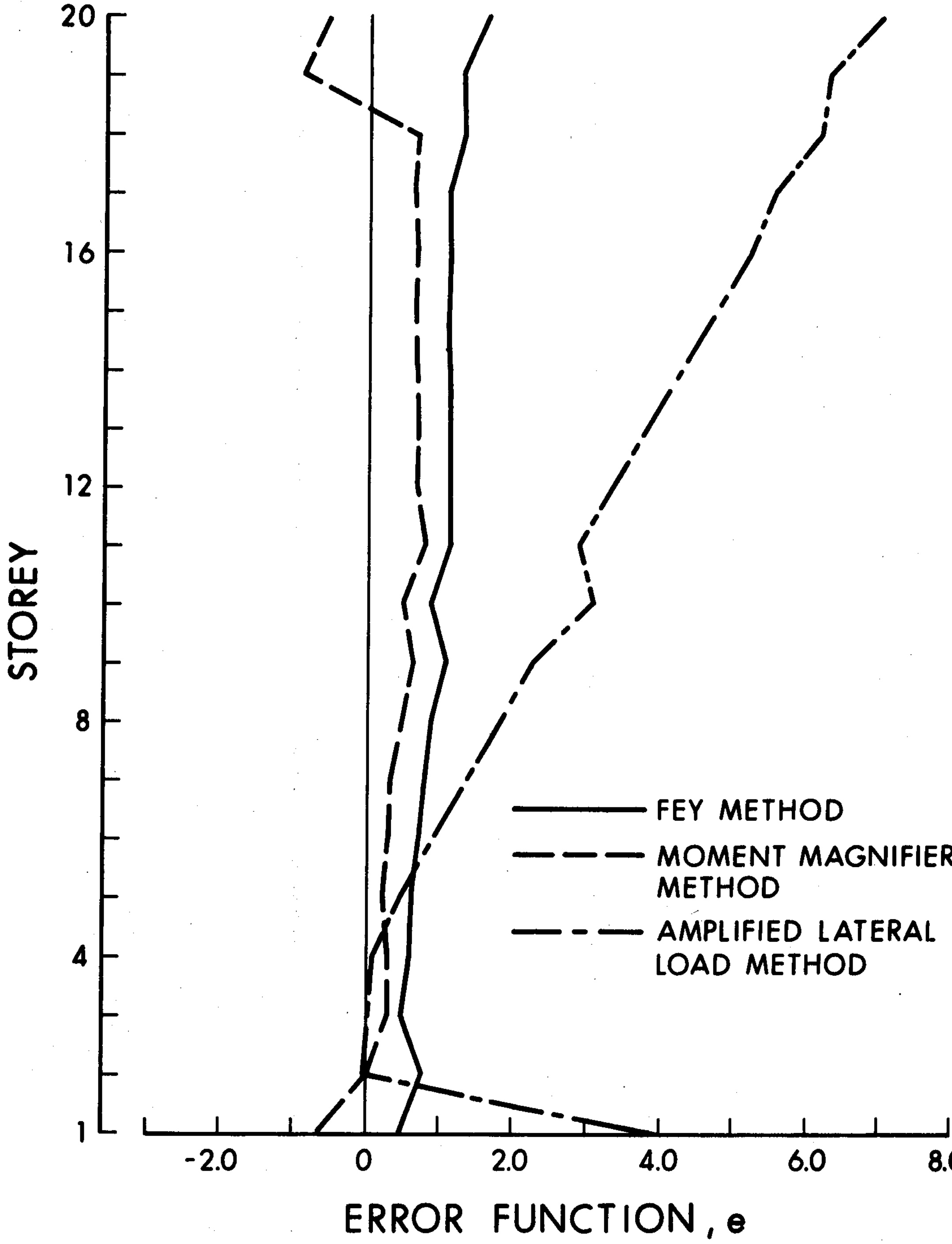

FIGURE 4.4 MOMENT ERRORS IN FRAME TYPE THREE

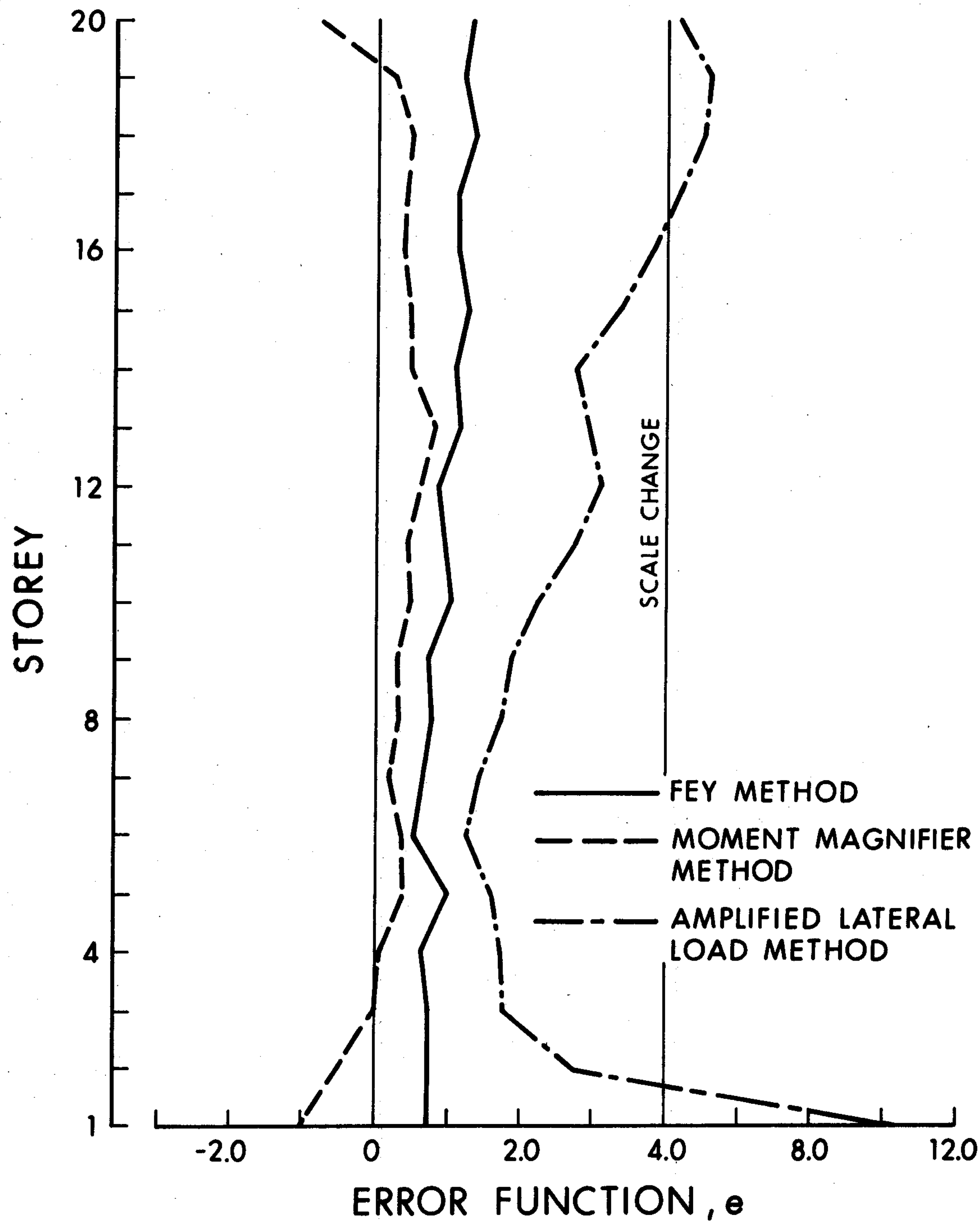

FIGURE 4.5 MOMENT ERRORS IN FRAME TYPE FOUR

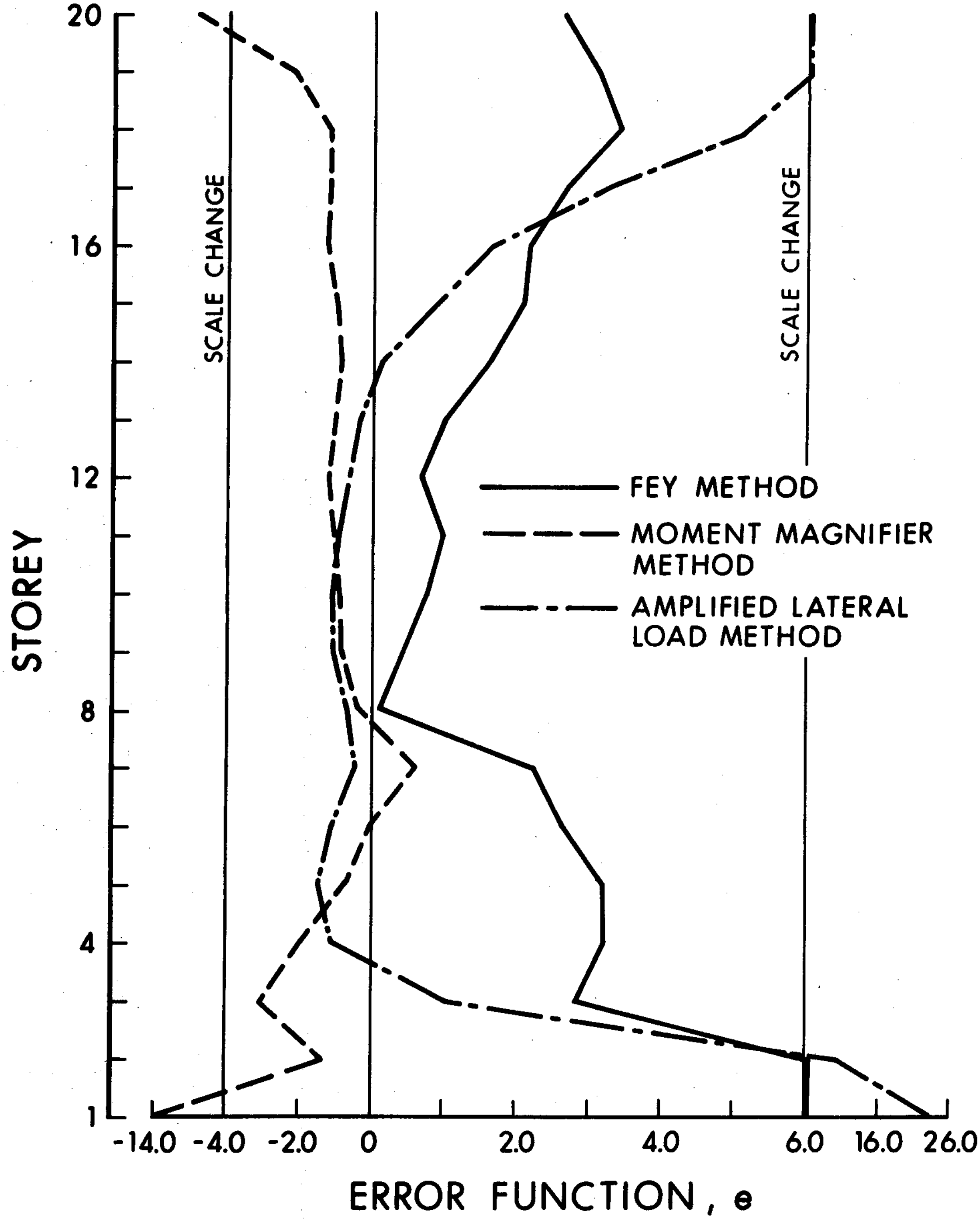

FIGURE 4.6 MOMENT ERRORS IN FRAME TYPE FIVE

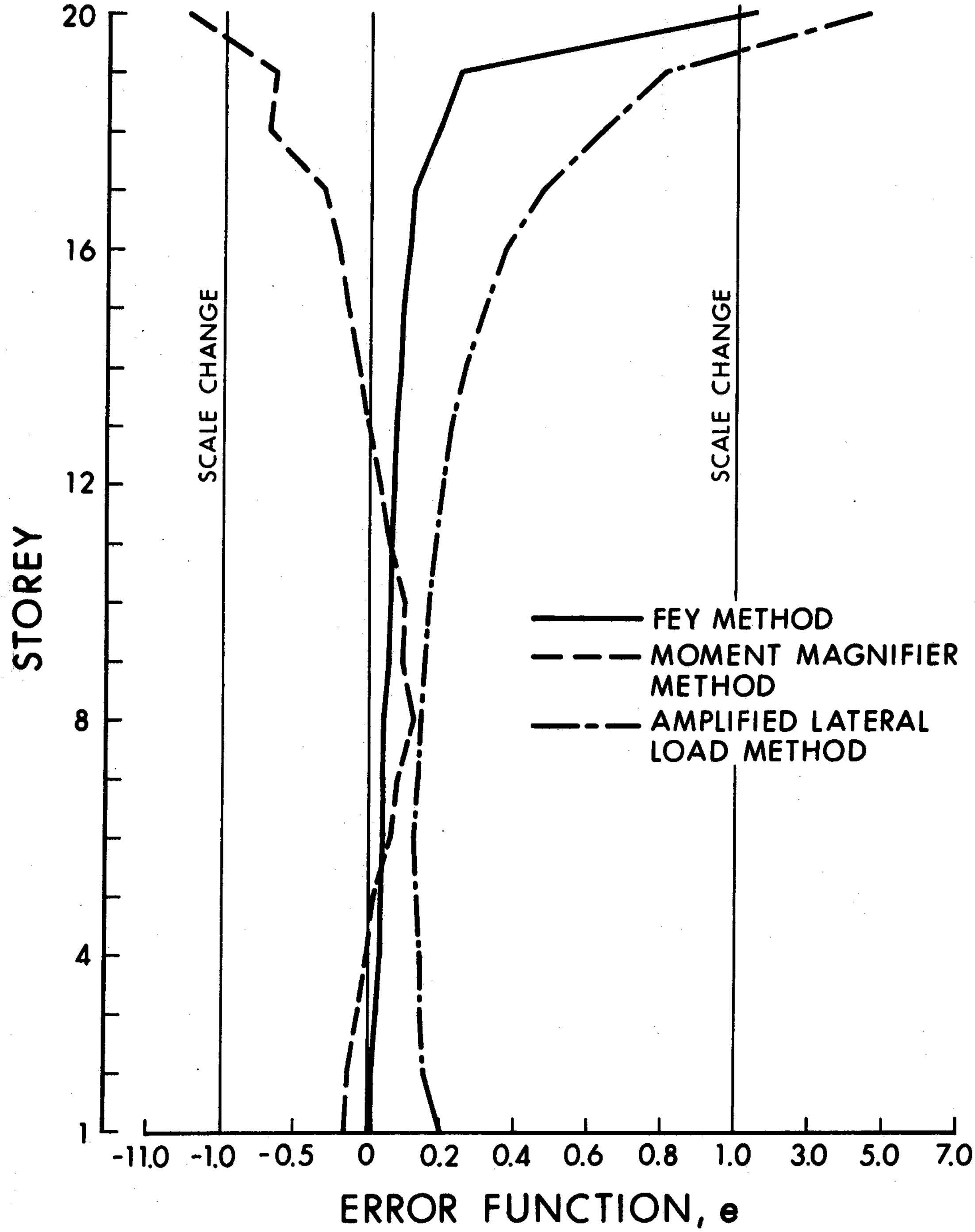

FIGURE 4.7 MOMENT ERRORS IN FRAME TYPE SIX

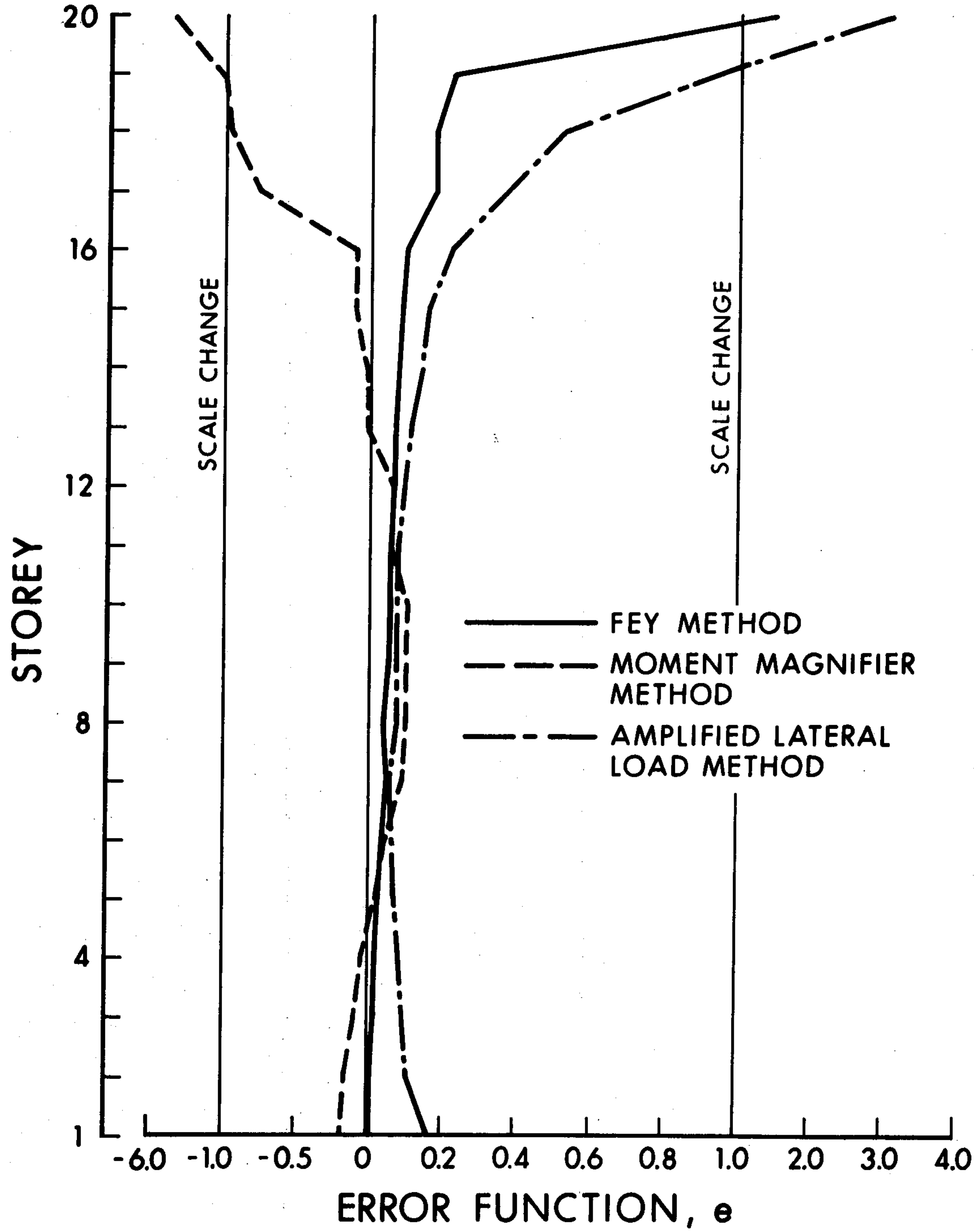

FIGURE 4.8 MOMENT ERRORS IN FRAME TYPE SEVEN

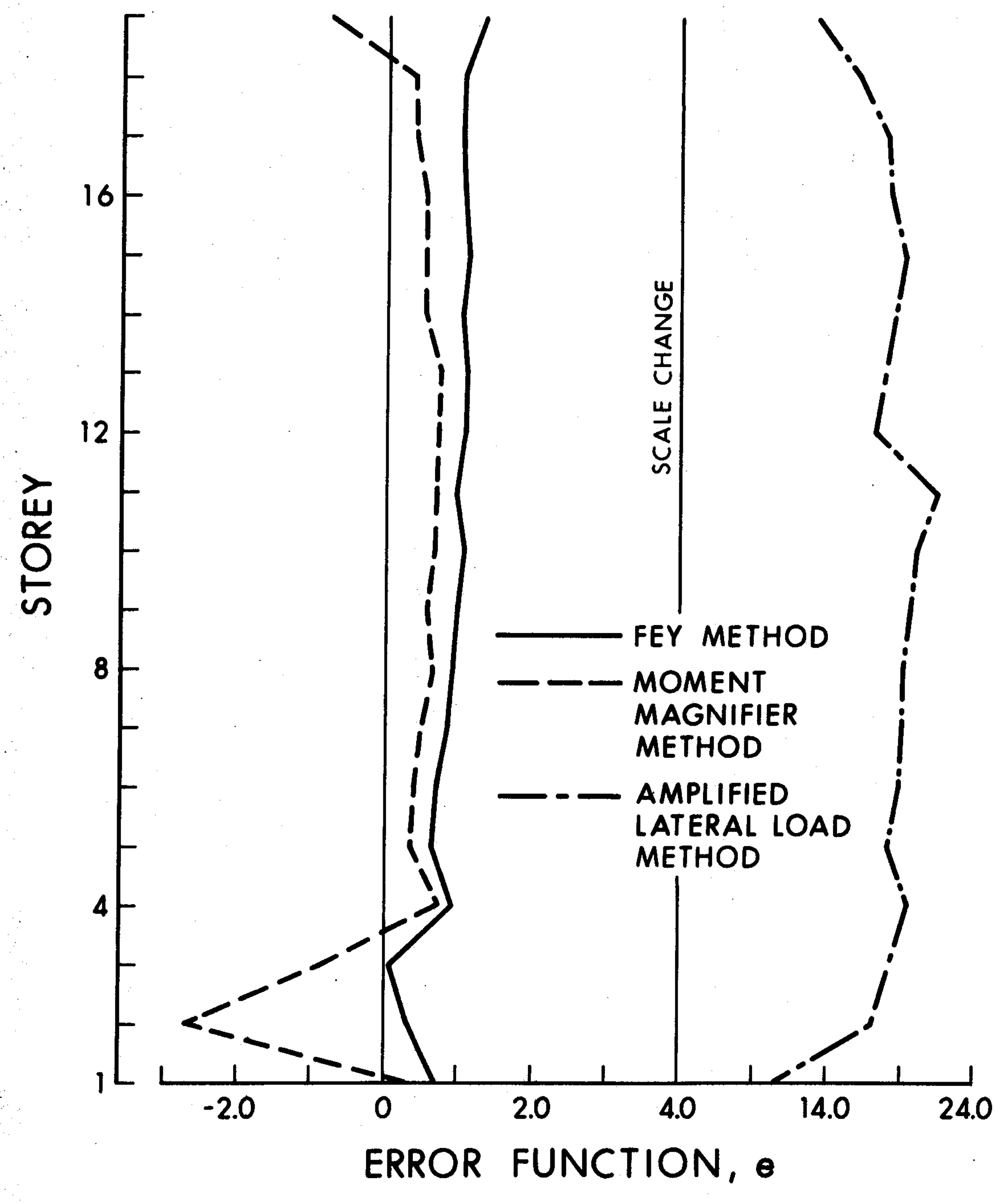

FIGURE 4.9 MOMENT ERRORS IN FRAME TYPE EIGHT

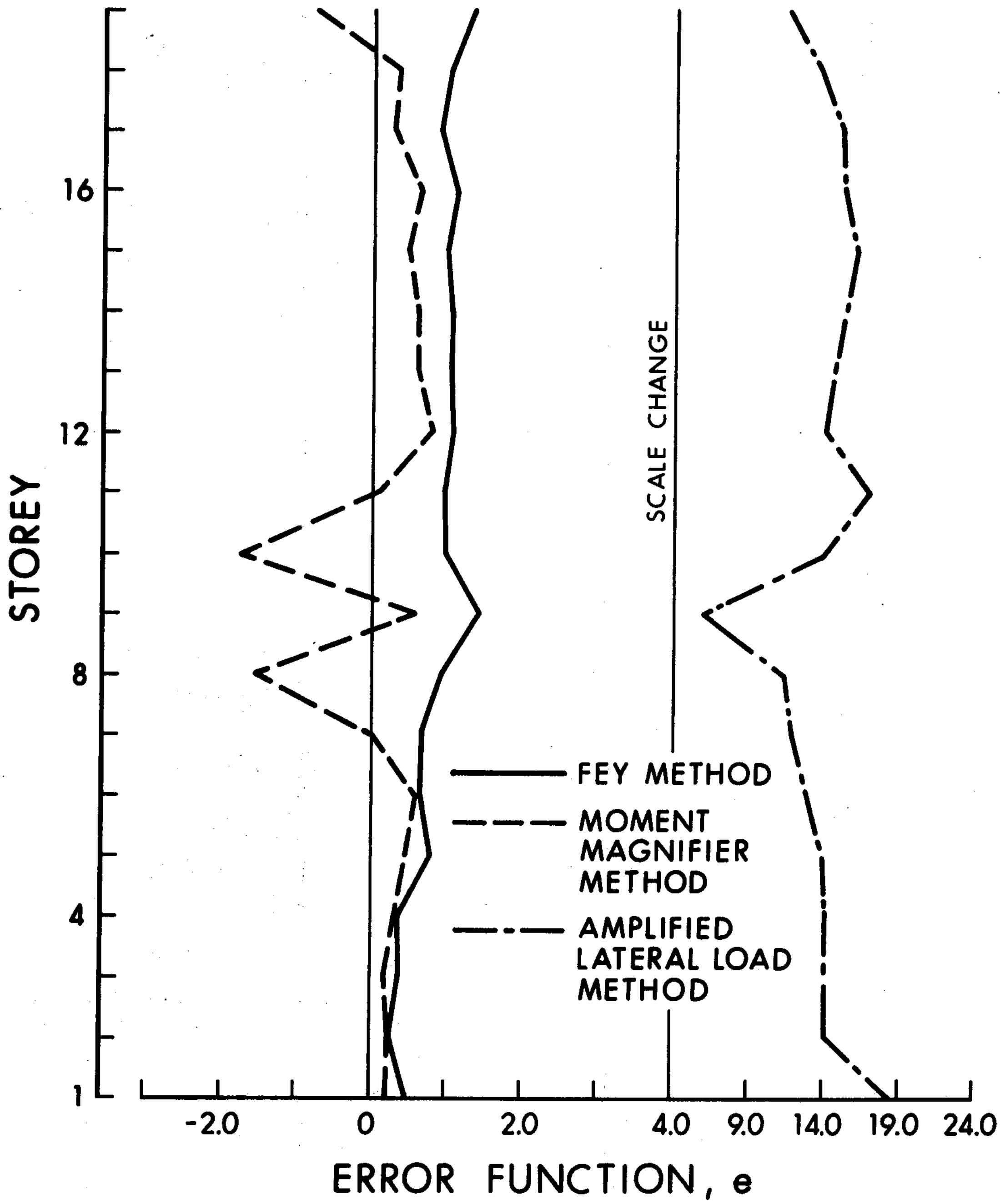

FIGURE 4.10 MOMENT ERRORS IN FRAME TYPE NINE

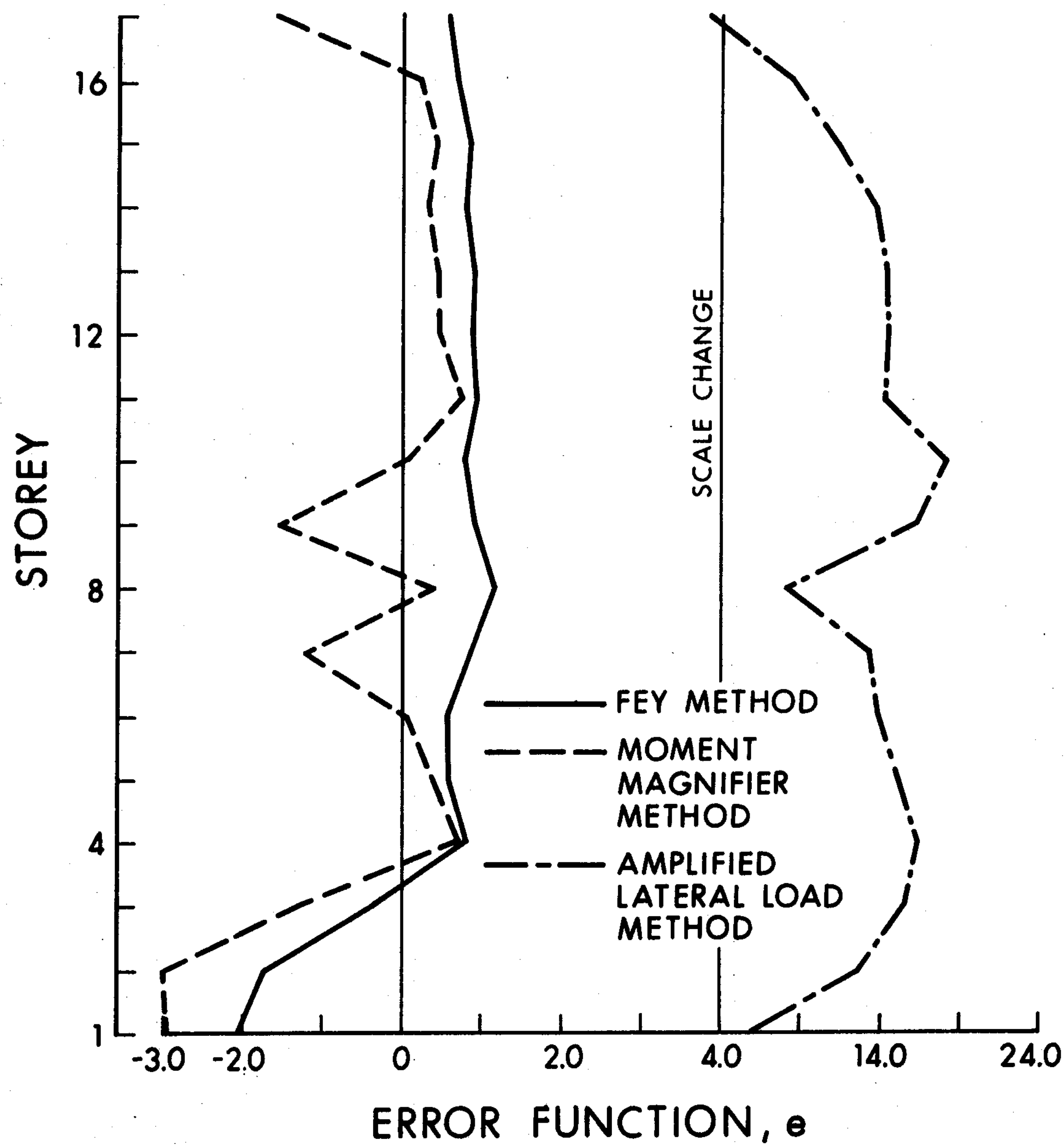

FIGURE 4.11 MOMENT ERRORS IN FRAME TYPE TEN

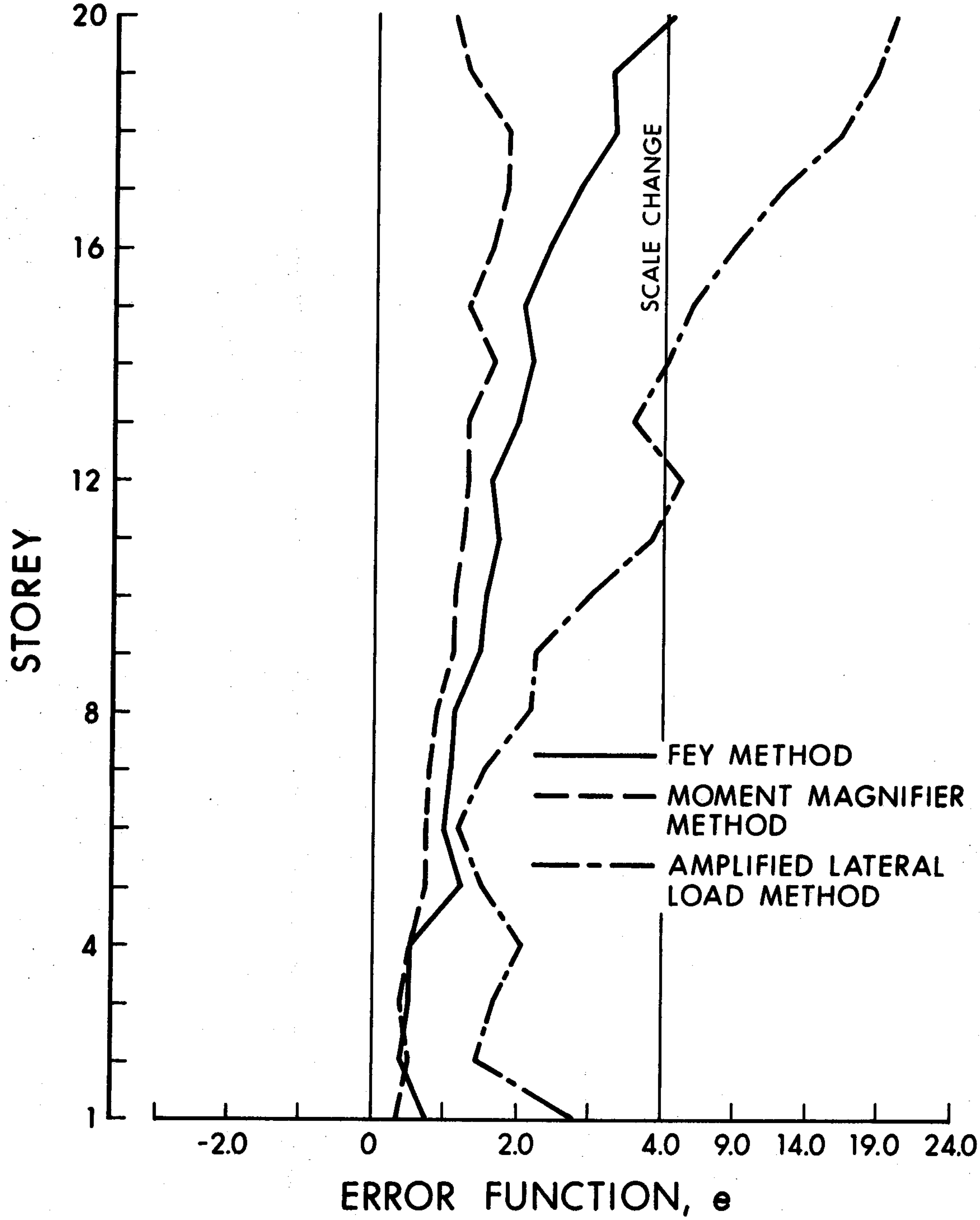

FIGURE 4.12 MOMENT ERRORS IN FRAME TYPE ELEVEN

CHAPTER 5

COLUMN DESIGN FOLLOWING SECOND-ORDER ANALYSIS

5.1 Introduction

Figure 5.1 shows columns with and without lateral displacements of the ends. If translation is prevented, the deflected shape is as shown in Figure 5.1(a). The moments M_T and M_B are the applied end moments while M_{RT} and M_{RB} are restraining moments caused by the rotations of the end restraints as the column deflects. Horizontal forces, H, are present if the end moments are unequal. At mid-height there are secondary moments equal to the axial load times the deflection shown shaded. To account for the restraining moments M_{RT} and M_{RB} in the design of this braced column an effective length less than the real length is used to compute the lateral deflections.

If, however, the column is free to sway laterally as shown in Figure 5.1(b), the moments M_T and M_B must equilibrate not only any horizontal load, H, but also a moment $P\Delta$. The secondary moments in this column can be divided into two components, one due to the additional horizontal reaction or sway force, $P\Delta/h$, necessary to resist the axial force in the deformed position, and the second equal to the axial load times the deflection from the chord line, shown shaded in Figure 5.1(b). Traditionally these have both been accounted for in design by using the elastic effective length factors for the unbraced case in designing the column.

On the other hand, if a second-order structural analysis is carried out including the effects of both the applied loads and the sway forces, the latter have been accounted for in the analysis and

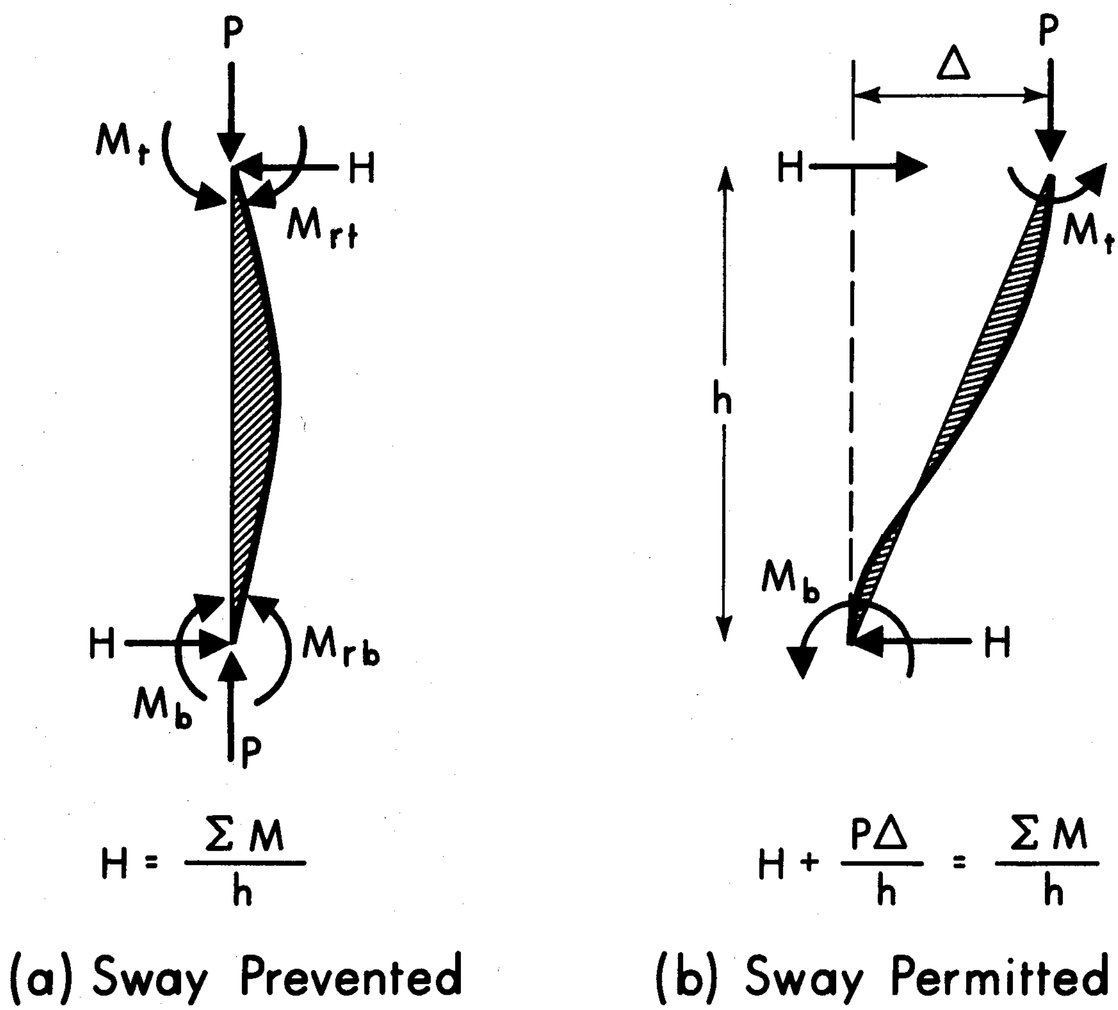

FIGURE 5.1 FORCES IN DEFLECTED COLUMN

need not be considered a second time in evaluating the effective length. Since the maximum moment theoretically may occur away from the ends of the column it may be necessary to use a moment magnifier calculation to estimate this moment. A procedure for determining whether such a magnification is required is presented in section 5.2, and the necessary values of the effective length factor, K, and the equivalent moment factor, C_m, are discussed in section 5.3. The proposed column design procedure is compared in section 5.4 to the second-order column moments in a one storey frame and to 10 columns selected from the 11 frames analyzed in Chapter 4.

5.2 Test of Whether Maximum Column Moment Occurs at End of Column

Galambos[(6)] shows that the maximum moment in an elastic beam-column loaded with an axial load and end moments M_a and M_b is:

$$M_{MAX} = \delta M_a \qquad 5.1$$

$$\delta = \frac{\sqrt{1 + (M_b/M_a)^2 - 2(M_b/M_a)\cos\alpha}}{\sin\alpha} \qquad 5.2$$

where M_a = larger end moment in the column, always positive.

M_b = smaller end moment in the column, positive if column is bent in single curvature.

$\alpha = h\sqrt{P/EI} = \pi\sqrt{P/P_E}$

P_E = Euler load $= \dfrac{\pi^2 EI}{h^2}$

MacGregor[(11)] has used these equations to derive a test for determining whether a given column can be designed for the maximum end moment, M_a, or whether the moments between the ends of the column will exceed those at the ends. If it is assumed that stability effects can be disregarded if M_{MAX} is not more than 1.05 M_a, Equation 5.2 can be solved to determine the combinations of M_b/M_a and α corresponding to δ = 1.05. These are plotted with the solid line for δ = 1.05 in Figure 5.2. Columns represented by combinations of M_b/M_a and α^2 falling below this line can be designed for the second-order end moments without a further moment magnification. This line can be approximated by the equation shown in Figure 5.2. Thus if:

$$\frac{M_b}{M_a} < (1.1 - \frac{P_u L^2}{3EI}) \qquad 5.3$$

The maximum moment will always be less than 1.05 times that at the end of the column.

5.3 Derivation of K-Factor

If Equation 5.3 shows that the maximum column moment occurs away from the end of the column, column design should be based on amplified moments based on the ACI moment magnifier with the equivalent moment factor, C_m, taken for the braced frame case using the ratio of end moments obtained from the second-order analysis, and with the effective length factor K = 1.0. This can be demonstrated by setting the moment magnifier from Equation 5.2 equal to the ACI moment magnifier given as:

$$\delta = \frac{C_m}{1 - \frac{P_u}{P_{cr}}} \qquad 5.4$$

where, P_u is the ultimate load on the column and P_{cr} the critical load equal to $\pi^2 EI/(KL)^2$.

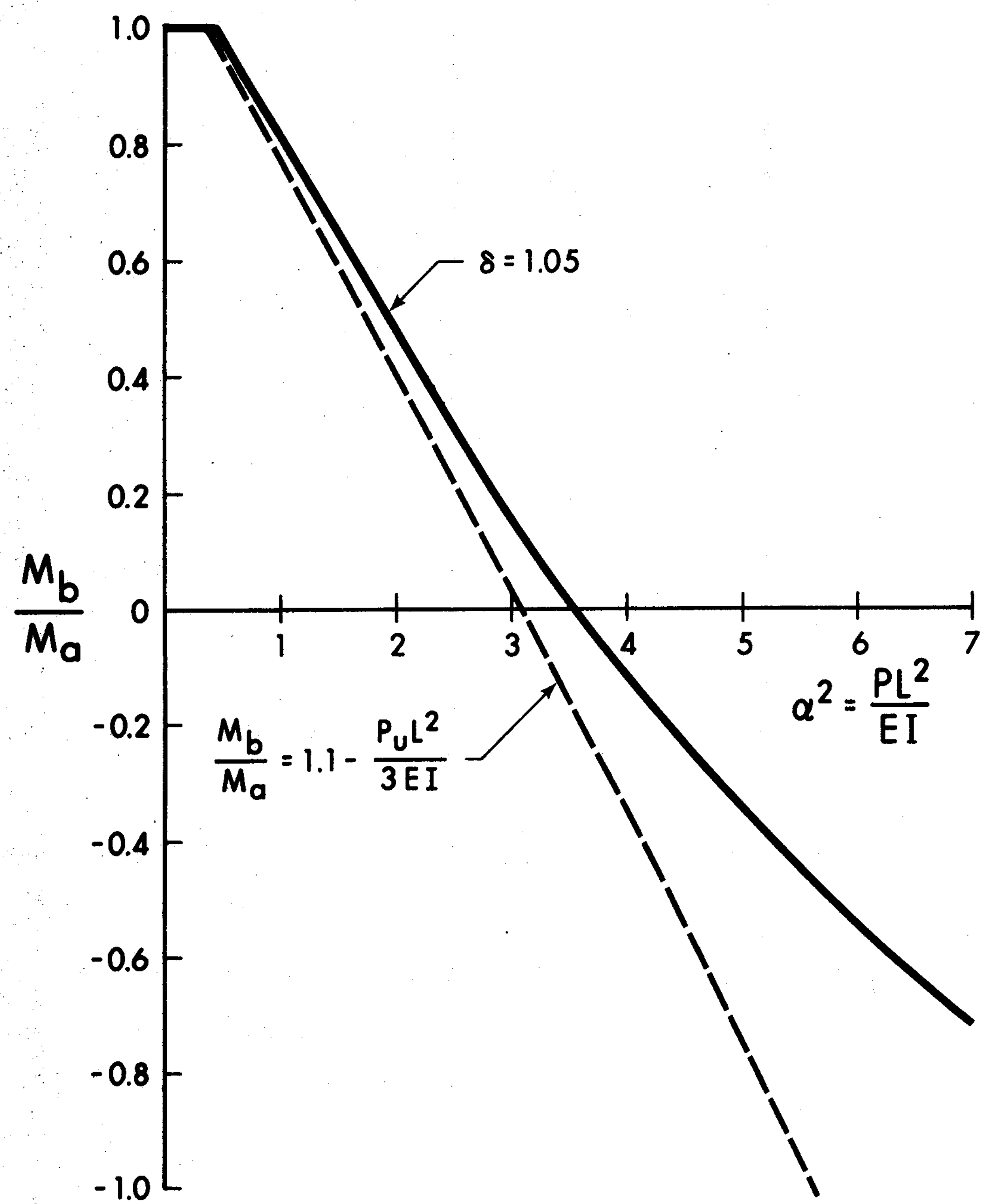

FIGURE 5.2 LIMITS ON COLUMNS WITH MAXIMUM MOMENT AT END OF COLUMN

and

$$C_m = 0.6 + 0.4 \frac{M_b}{M_a} \qquad 5.5$$

Equating Equations 5.2 and 5.4 gives:

$$\frac{C_m}{1 - \frac{K^2\alpha^2}{\pi^2}} = \frac{\sqrt{1 + (M_b/M_a)^2 - 2(M_b/M_a)\cos\alpha}}{\sin\alpha} \qquad 5.6$$

which reduces to:

$$K = \frac{\pi}{\alpha}\sqrt{1 - \frac{C_m \sin\alpha}{\sqrt{1 + (M_b/M_a)^2 - 2(M_b/M_a)\cos\alpha}}} \qquad 5.7$$

Equation 5.7 was solved for values of M_b/M_a from -1 to +1 and P/P_E from 0.03 to 0.63. The values of K computed using Equation 5.7 ranged from 0.999 to 1.265. The values of K greater than 1.10 corresponded to cases where C_m is underestimated by the ACI equation (columns with α and M_b/M_a both low. See Reference 20.) If these values were excluded, the average K value was equal to 1.05. The absence of any K values less than 1.0 indicates that the braced frame effective lengths should not be used if the column end moments are known from a second-order analysis.

5.4 Verification of Design Procedure

To verify the column design procedure, presented in sections 5.2 and 5.3, the frame of Figure 5.3 was analyzed with a negative bracing member. The loading was as shown and the column under consideration was broken into four equal length segments to allow calculation of the deflections and moments at points between the ends of the column.

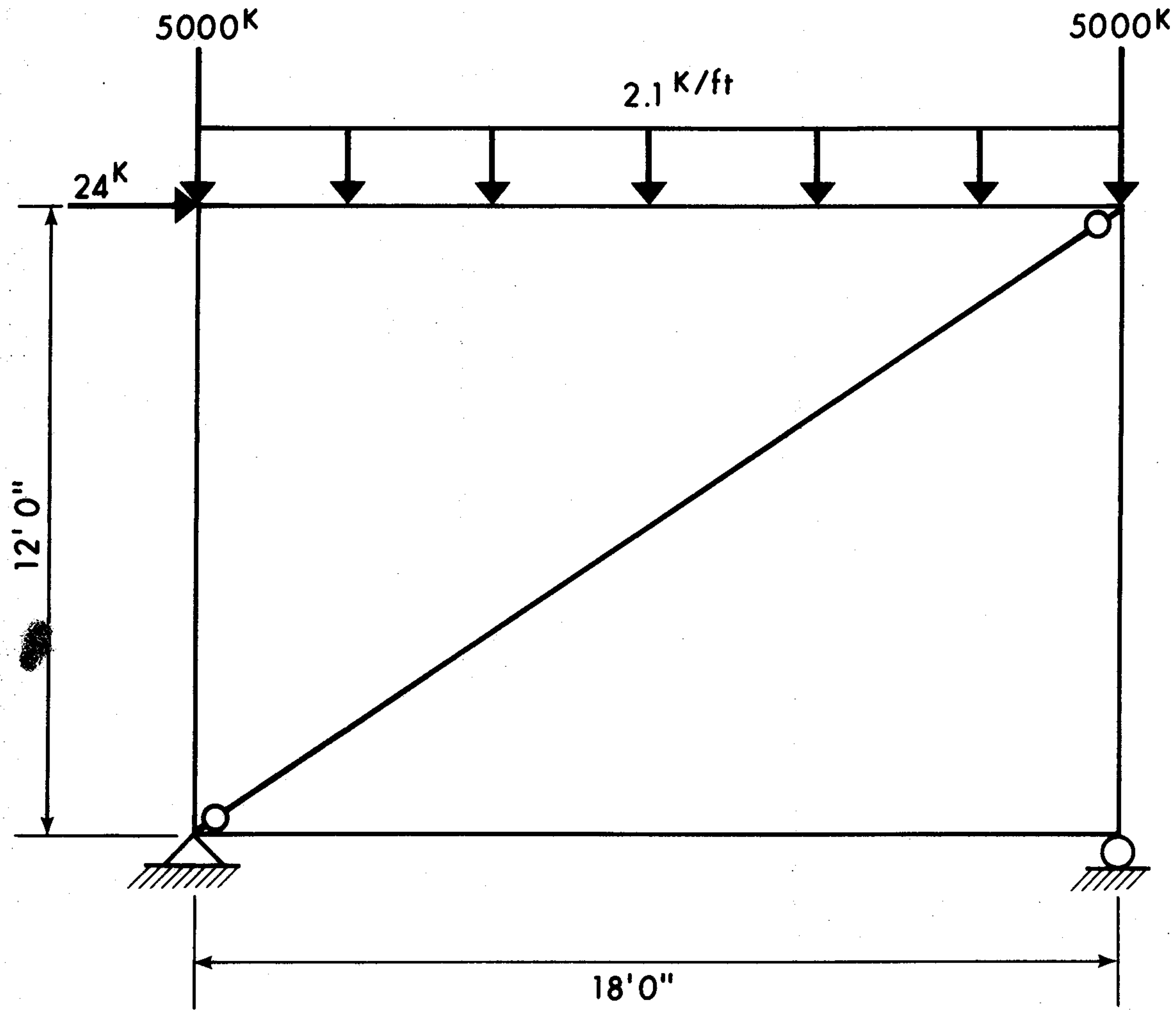

FIGURE 5.3 TEST FRAME

The frame was assumed to be constructed of normal weight concrete with a strength of 4000 psi and elastic modulus as given by Equation 3.1. The column and beam moments of inertia were 15617 in^4 and 16384 in^4, respectively. The negative brace area was given by Equation 2.17.

Initially, the frame was analyzed as shown in Figure 5.3 to obtain deflections and end moments in the windward column. From the resulting deflections it was possible to calculate the relative deflection from a chord line joining the upper and lower ends of the column. The frame was then reanalyzed under the same loading but with the node points in the position resulting from the first cycle. Three cycles were required to obtain convergence. The moments in the windward column of the frame are shown in Figure 5.4. During the iterations the moments at mid-height of the column increased and those at the ends decreased. The decrease in the end moments occurred because the lateral deflections caused a slight decrease in the stiffness of the column.

Equation 5.3 may now be used to test whether design of the column may be based on the larger end moment or whether a magnification is required. The ratio of column end moments is found to be:

$$\frac{M_b}{M_a} = \frac{15.3}{15.4} \simeq 1.0$$

The right-hand-side of Equation 5.3 is:

$$1.1 - \frac{P_u L^2}{3EI} = 1.1 - \frac{(5016\ K) \times (144\ in)^2}{3 \times 3605\ ksi \times 15617\ in^4}$$

$$= 0.48$$

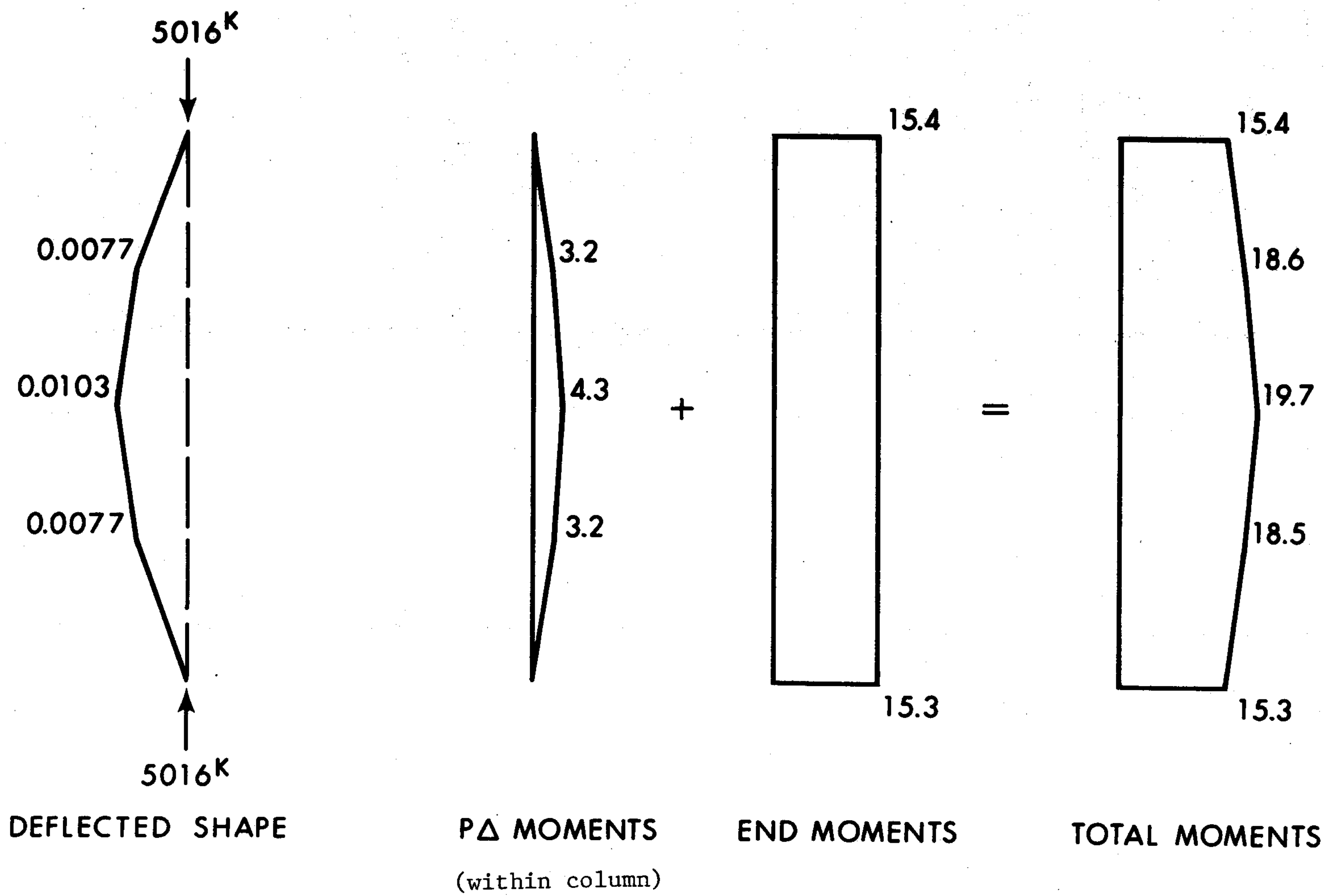

FIGURE 5.4 DEFLECTIONS AND MOMENTS IN WINDWARD COLUMN

Hence, the test shows that the maximum moment occurs between the ends of the column and design must be based on an amplified moment.

Design of this column by the ACI code would require calculating M_{MAX} as given by Equation 5.1.

For the frame of Figure 5.3, based on the second-order end moments from the third cycle of iteration, C_m would be:

$$C_m = 0.6 + 0.4\left(\frac{15.3}{15.4}\right) = 1.0$$

The critical buckling load assuming an effective length factor equal to 1.0 would be:

$$P_{cr} = \frac{(3.14)^2 \times 3605 \text{ ksi} \times 15617 \text{ in}^4}{(1.0 \times 144 \text{ in})^2} = 26769 \text{ K}$$

Solving Equation 5.4 for the moment magnifier gives:

$$\delta = \frac{1.0}{1 - \frac{5016K}{26769K}} = 1.23$$

Finally, the column design moment would be given by Equation 5.1 as:

$$M_{MAX} = 1.23 \times 15.4 \text{ ft-K} = 18.9 \text{ ft-K}$$

This compares to a maximum column moment of 19.7 ft-K from the iterative analysis. Thus, the ACI procedure with K = 1.0 underestimated the maximum column moment by 3.8 per cent. Had the braced frame effective length of 0.81 been used in the calculations, the magnified moment would be estimated as 17.6 ft-K or 10.9 per cent low. This suggests that the hinged end effective length (K = 1.0) gives a better estimate of the magnification than the braced effective length.

A number of columns were chosen from the eleven frames studied in Chapter four to further check this design method. Table 5.1

gives the second-order end moments of ten single curvature columns and the ultimate vertical load on the storey where that column is located. In calculating the second-order moments along the columns the total vertical storey load was artificially assumed to act on the column in question to represent an extreme hypothetical condition for which the second-order frame analysis was applicable. As shown in Table 5.1, Equation 5.3 indicated that six of the ten columns required additional moment magnification to estimate the maximum moments in the columns.

The moments computed using a moment magnifier analysis are compared in Table 5.2 to those from the second-order analysis. In both calculations the entire axial load was assumed to act on the column in question. It can be seen that columns one, five, six and eight, which Equation 5.3 identified as not requiring additional moment magnification, indeed did not need moment magnification. All the columns identified as requiring moment magnification, did need magnification except column ten which was marginal but did not require magnification.

The values of the maximum column moment in Table 5.2 computed using K = 1.0 were conservative in all cases while those based on the braced frame K were unconservative in all cases when compared to the column moments computed in one cycle of iteration by the procedure described earlier. This supports the observation that if the column end moments are known from a second-order analysis, the effective length factor should be taken as K = 1.0 and the equivalent moment factor, C_m, should be based on the braced frame case.

TABLE 5.1 Application of Equation 5.3 to Single Curvature Columns from Frames Analyzed

No.	Frame Type	Storey	$P_{u,storey}$	M_b	M_a	M_b/M_a	$1.1 - \frac{P_u L^2}{3EI}$	Magnif. Req'd?
1	4	1	5729	23.6	182.9	0.13	0.40	NO
2	5	1	6323	45.6	70.9	0.64	0.32	YES
3	5	2	5972	14.8	23.7	0.62	0.37	YES
4	6	1	48433	78.3	159.5	0.49	-0.30	YES
5	8	2	4982	25.1	165.1	0.15	0.49	NO
6	9	10	2666	19.1	51.9	0.37	0.37	NO
7	9	8	3279	31.3	42.8	0.73	0.51	YES
8	10	9	2424	16.6	51.7	0.32	0.44	NO
9	10	7	3037	31.3	39.3	0.80	0.55	YES
10	11	10	4160	1.0	7.6	0.13	-0.03	YES

TABLE 5.2 Comparison of Moments Computed Using Moment Magnifier to Second-Order Moments

No.	M_{MAX} Actual	K = 1.0			K < 1.0		
		δ	M_{MAX}	Error	δ	M_{MAX}	Error
1	182.9	1.0*	182.9	0.0	1.0*	182.9	0.0
2	78.1	1.13	80.1	+2.6	1.0	70.9	-9.2
3	25.6	1.09	25.8	+0.8	1.04	24.6	-3.9
4	190.0	1.39	221.2	+16.4	1.00	159.5	-16.1
5	165.1	1.0*	165.1	0.0	1.0*	165.1	0.0
6	51.9	1.0*	51.9	0.0	1.0*	51.9	0.0
7	46.2	1.08	46.2	0.0	1.03	44.1	-4.5
8	51.7	1.0*	51.7	0.0	1.0*	51.7	0.0
9	42.8	1.10	43.2	+0.9	1.06	41.7	-2.6
10	7.6	1.0*	7.6	0.0	1.0*	7.6	0.0

* Maximum moment at end of column.

CHAPTER 6

SUMMARY AND CONCLUSIONS

In this study a column design method, based on a second-order analysis, was proposed. It was shown that the maximum moment in a single curvature column could be estimated by applying a moment magnifier to the larger end moment.

Results indicated that the effective length used in calculating the moment magnifier be taken equal to the actual column length. The use of the braced frame effective length gave approximations to the maximum column moment which were unconservative.

Three approximate methods of second-order analysis were presented and applied to eleven different building frames.

The Fey method and the moment magnifier method were shown to give essentially acceptable approximations to an "exact" second-order analysis. The amplified lateral load method, however, was grossly conservative in some of the cases studied, but became comparable to the Fey method and moment magnifier method for the stiffer frames. Difficulties also arose in this method if the sway deflection angles varied significantly from storey to storey.

REFERENCES

1. Adams, P.F., "Design of Steel Beam-Columns", Paper presented at the Canadian Structural Engineering Conference 1972, Canadian Steel Industries Construction Council, Toronto, Canada.

2. Ketchum, M.S., "The Design of Steel Mill Buildings", 5th Edition, McGraw-Hill Book Co. Inc., New York, N.Y., 1932, pp. 91, 118.

3. Nixon, D., Beaulieu, D., and Adams, P.F., "Simplified Second-Order Frame Analysis", Canadian Journal of Civil Engineering, Vol. 12, No. 4, Dec. 1975, pp. 602-605.

4. Aas-Jakobsen, K., "Design of Slender Reinforced Concrete Frames", Report No. 48, Institut Für Baustatik ETH Zurich, Nov. 1973.

5. MacGregor, J.G., Breen, J.E., and Pfrang, E., "Design of Slender Concrete Columns", ACI Journal, Jan. 1970.

6. Galambos, T.V., "Structural Members and Frames", Prentice-Hall, 1968.

7. ACI Committee 318, "Building Code Requirements for Reinforced Concrete" (ACI 318-71), American Concrete Institute, Detroit, 1971.

8. Schwaighofer, J., and Microys, H.F., "Analysis of Shear Walls Using Standard Computer Programs", ACI Journal, Dec. 1969.

9. Hage, S.E., "The Second-Order Analysis of Reinforced Concrete Frames", M.Sc. Thesis, University of Alberta, Edmonton, Structural Engineering Report No. 49, October 1974.

10. Rosenblueth, E., "Slenderness Effects in Buildings", ASCE J., Structural Division 91, ST1, Jan. 1967, pp. 229-252.

11. MacGregor, J.G., Hage, S.E., "The Analysis and Design of Reinforced Concrete Frames For Stability", Submitted to ASCE for publication.

12. Wood, B.R., Beaulieu, D. and Adams, P.F., "Column Design by P-Delta Method", J. Structural Div., ASCE, Vol. 102, No. ST2, Feb. 1976, pp. 411-427.

13. Springfield, J., and Adams, P.F., "Aspects of Column Design in Tall Steel Buildings", ASCE, J. Struc. Div., Vol. 98, No. ST5, May 1972, pp. 1069-1083.

14. Kordina, K., "Discussion No. 3 - Cracking and Crack Control", Proc. Int. Conf. on Planning and Design of Tall Buildings, Lehigh University, Aug. 1972, Vol. III, pp. 721-722.

15. Beaufait, F.W., Rowan, W.H., Jr., Hoadley, P.G., and Hackett, R.M., 1970, "Computer Methods of Structural Analysis", Prentice-Hall, Englewood Cliffs, N.J..

16. Stevens, L.K., "Elastic Stability of Practical Multi-Storey Building Frames", Proc. ICE, 36, 1967, 99-117.

17. Fey, T., "Approximate Second-Order Analysis of Reinforced Concrete Frames", (in German), Bauingenieur, June 1966.

18. Goldberg, J.E., "Approximate Methods for Stability and Frequency Analysis of Tall Buildings", Proc. Conferencia Regional Sobie Edificios de Altura, Sept. 17-19, 1973, Madrid, pp. 123-146.

19. Parme, A.L., "Capacity of Restrained Eccentrically Loaded Long Columns", Symposium on Reinforced Concrete Columns, ACI Special Publication SP13, Detroit, 1966, pp. 355-360.

20. Wang, C.K., and Salmon, C.G., "Reinforced Concrete Design", 2nd Edition, In Text, 1973, p. 571.

21. Fintel, M., "Deflections of High-Rise Concrete Buildings", ACI Journal, Proc. Vol. 72, July 1975, p. 324.

APPENDIX A

COLUMN END MOMENTS FOR FRAMES STUDIED

A.1 Introduction

In this Appendix are tabulated all column end moments for each frame studied in this thesis. In each figure the upper right hand box attached to the column indicates the top end moment. The bottom end moment is listed in the lower left hand box. The first value in each box represents the "exact" second-order end moment. The second, third and fourth entries give the results of the Fey method, the moment magnifier method and the amplified lateral load method, respectively. The arrow associated with each box indicates the direction of the end moment on the column.

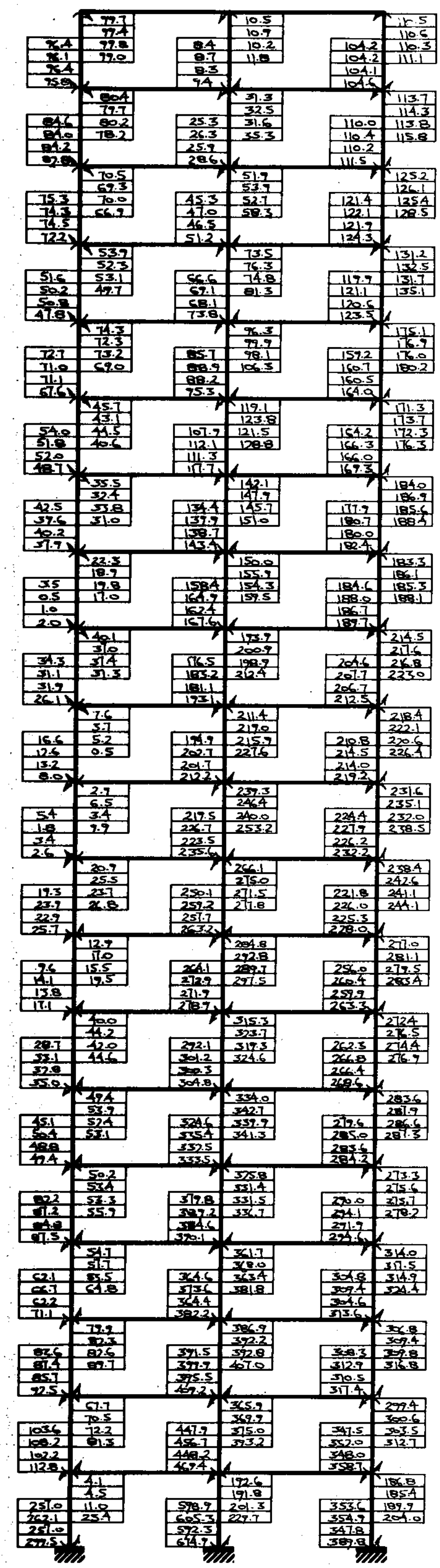

FIGURE A.1 FRAME TYPE ONE

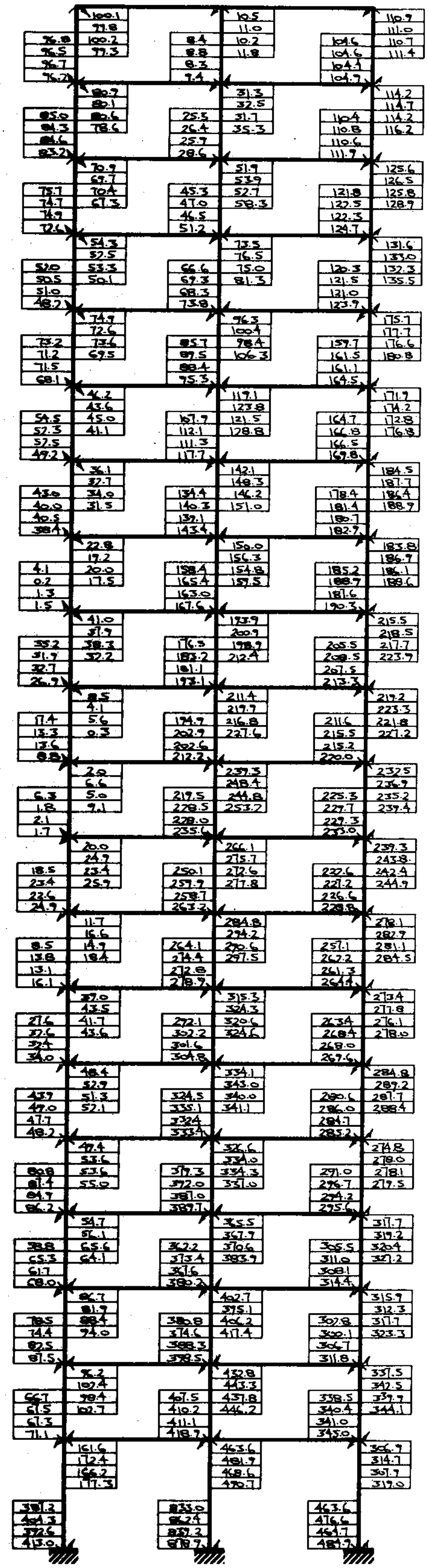

FIGURE A.2 FRAME TYPE TWO

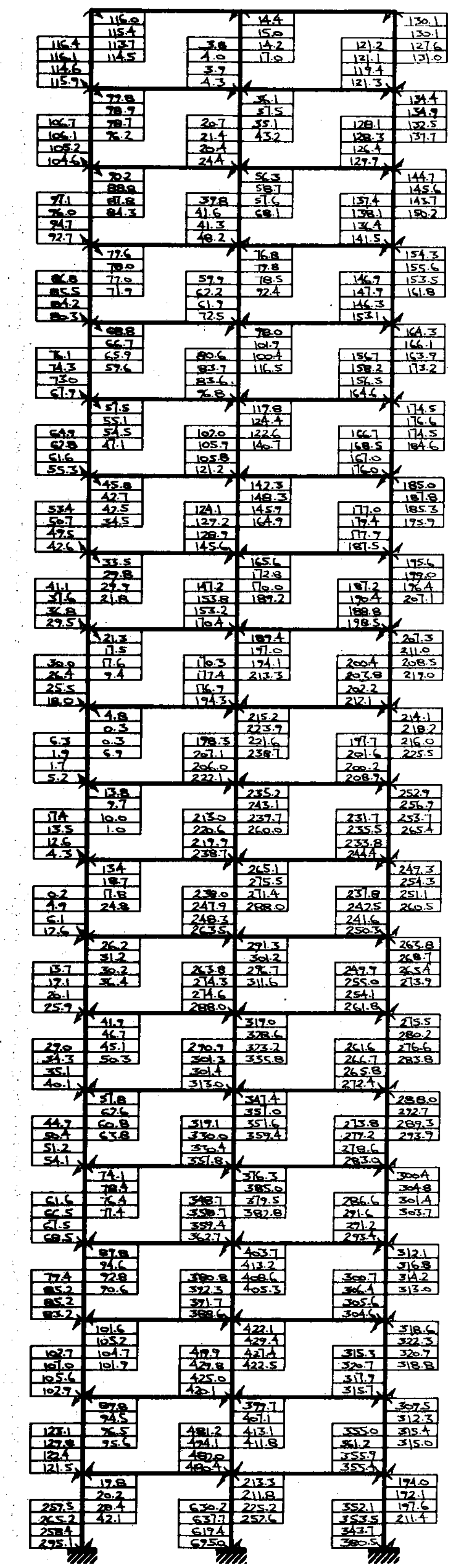

FIGURE A.3 FRAME TYPE THREE

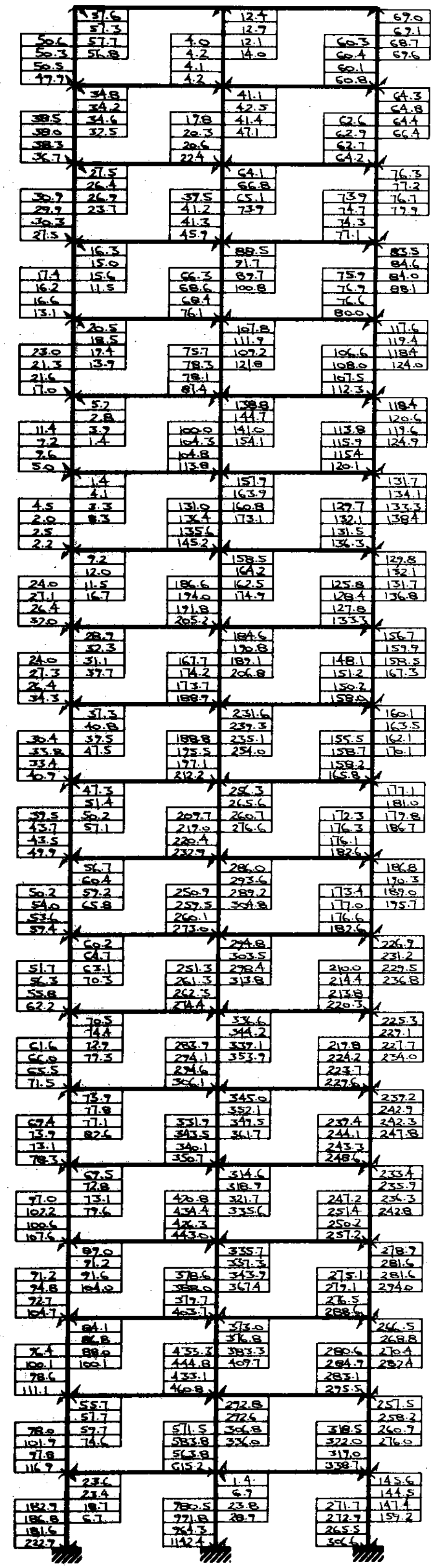

FIGURE A.4 FRAME TYPE FOUR

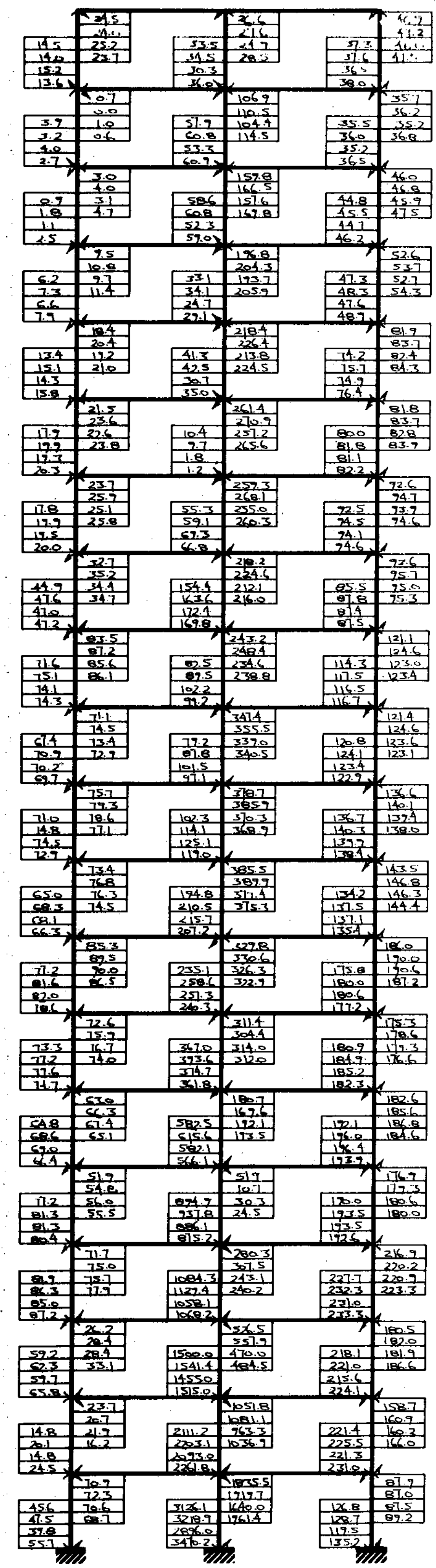

FIGURE A.5 FRAME TYPE FIVE

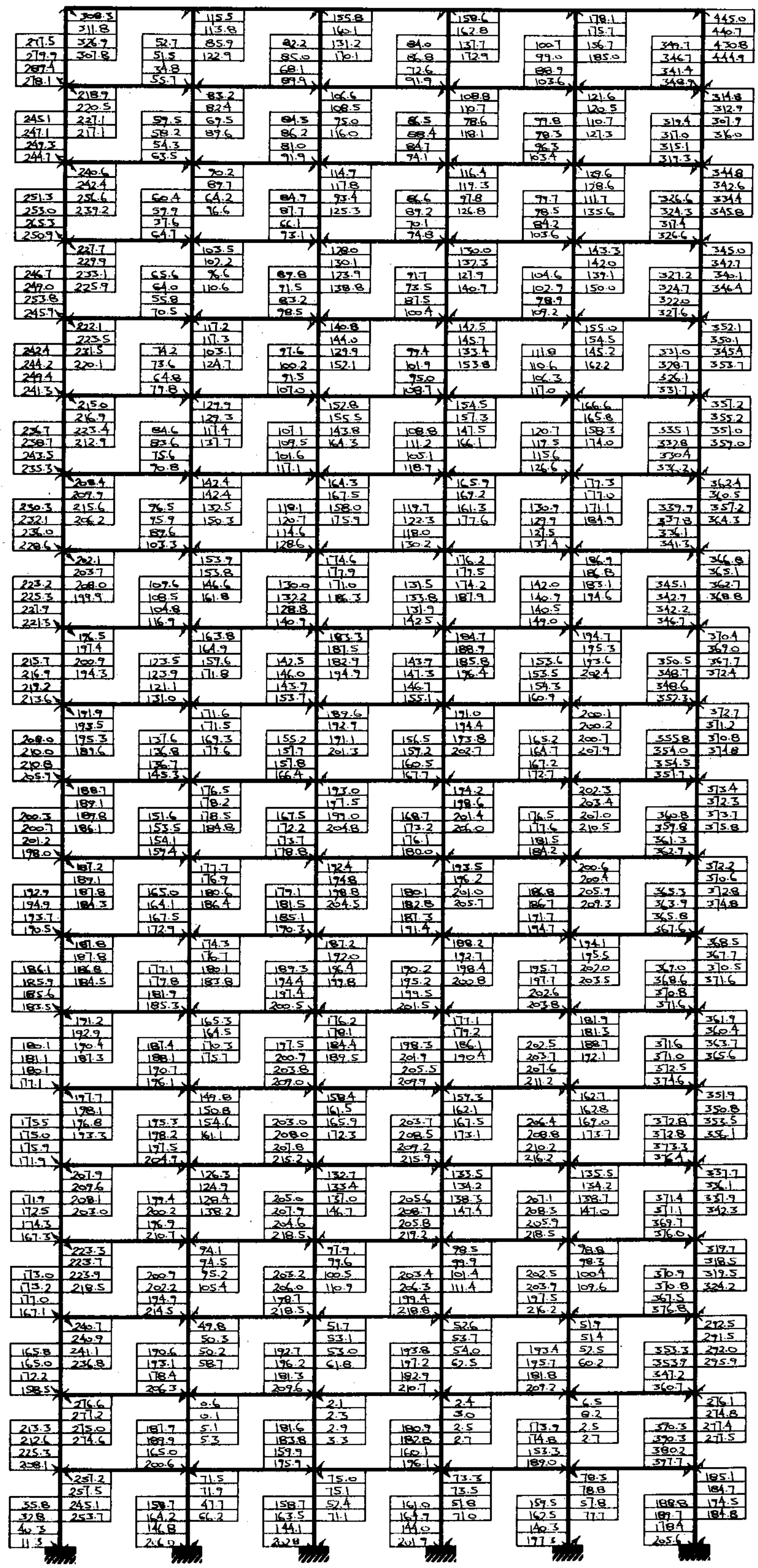

FIGURE A.6(a) FRAME TYPE SIX

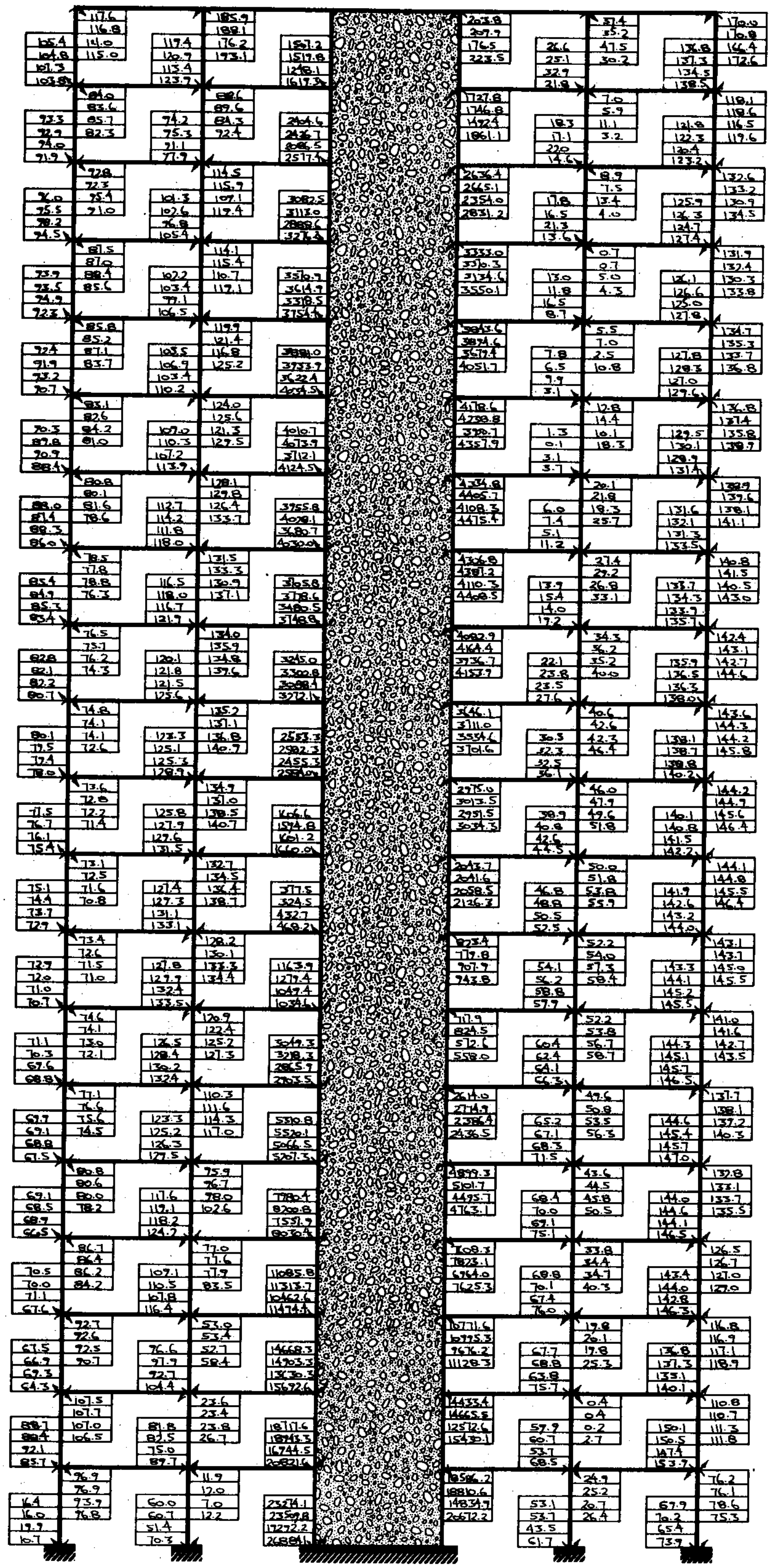

FIGURE A.6(b) FRAME TYPE SIX

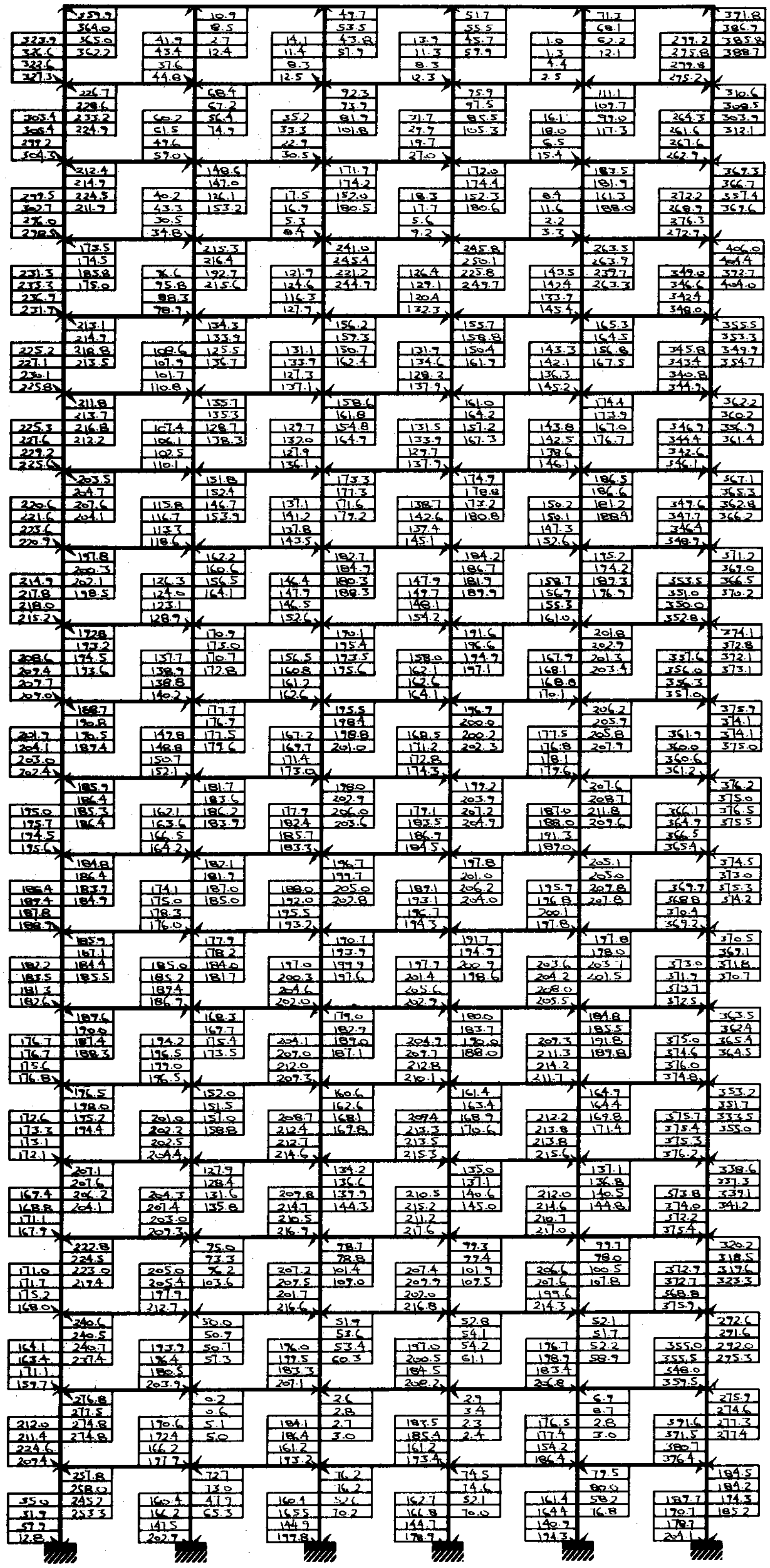

FIGURE A.7(a) FRAME TYPE SEVEN

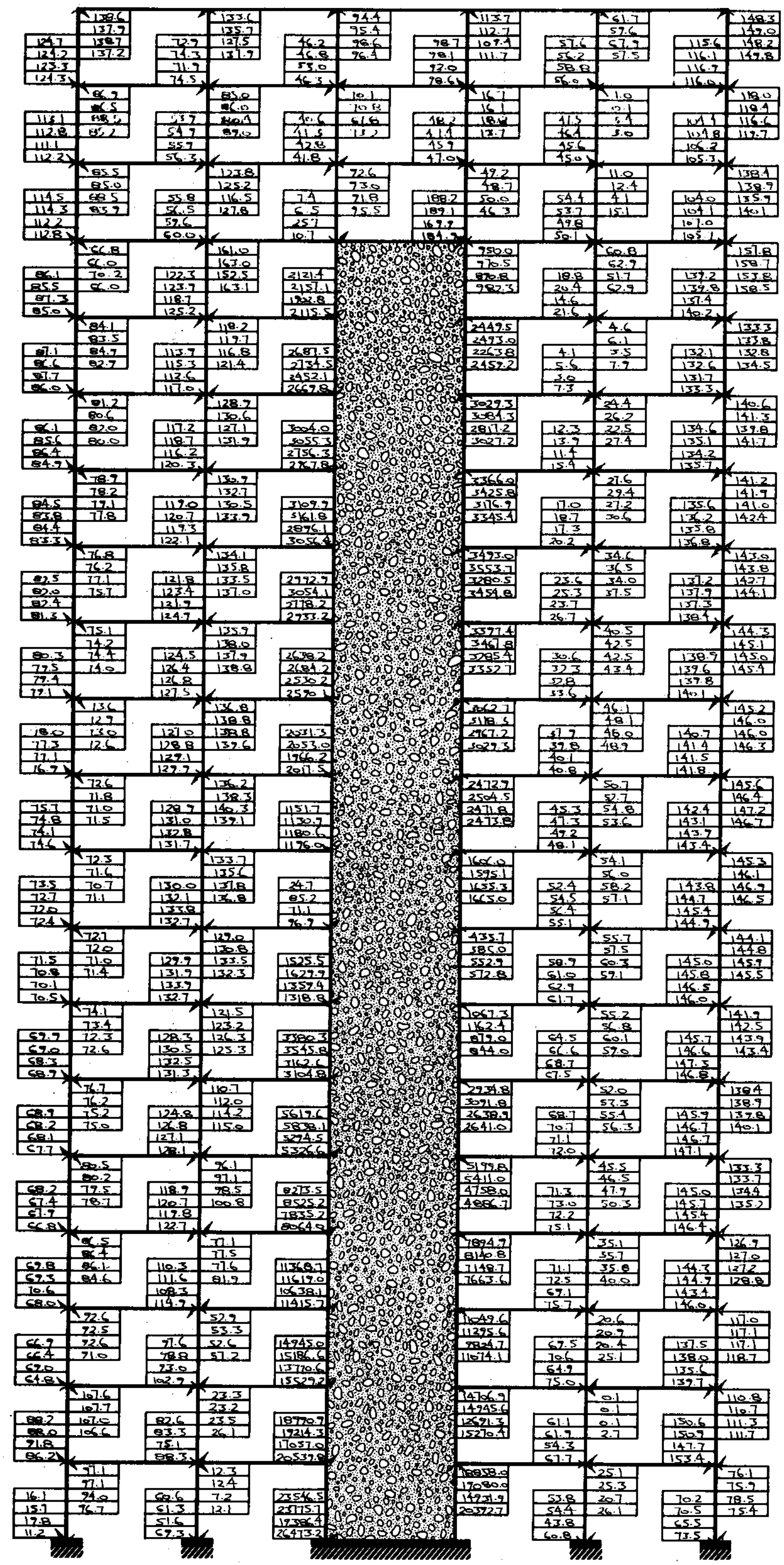

FIGURE A.7(b) FRAME TYPE SEVEN

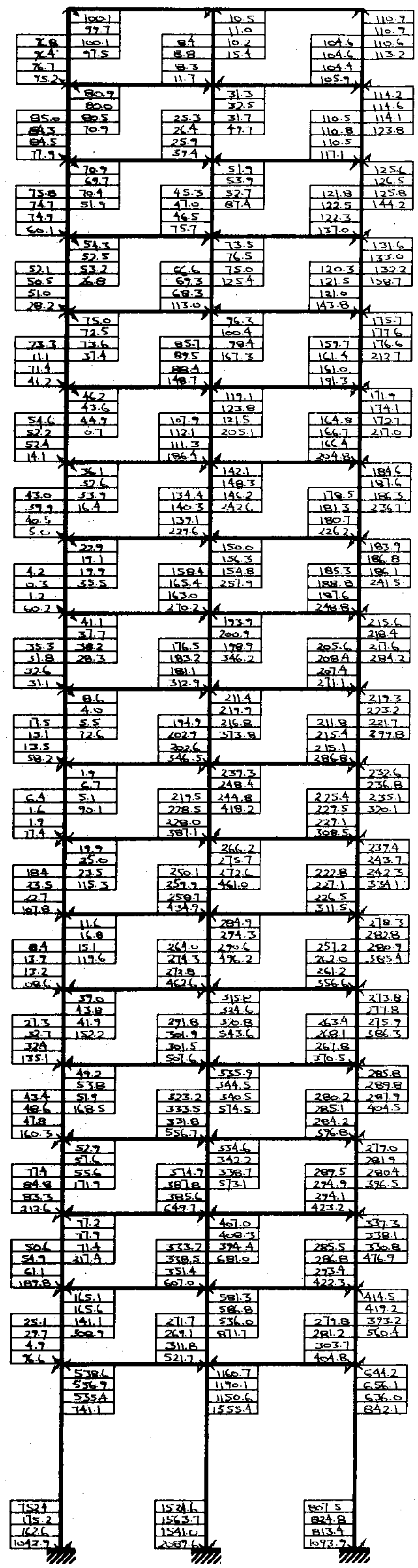

FIGURE A.8 FRAME TYPE EIGHT

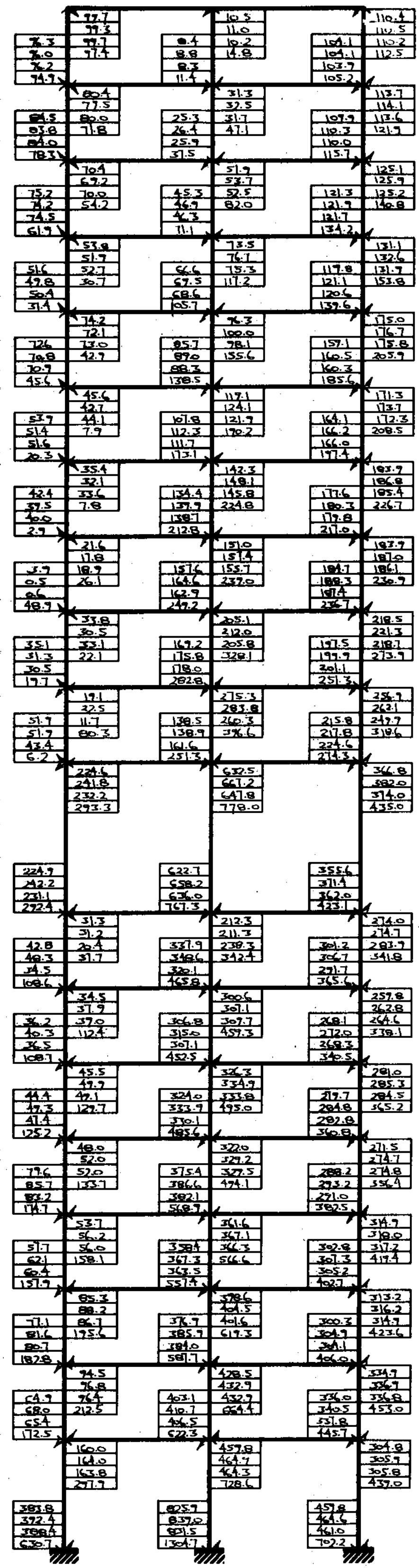

FIGURE A.9 FRAME TYPE NINE

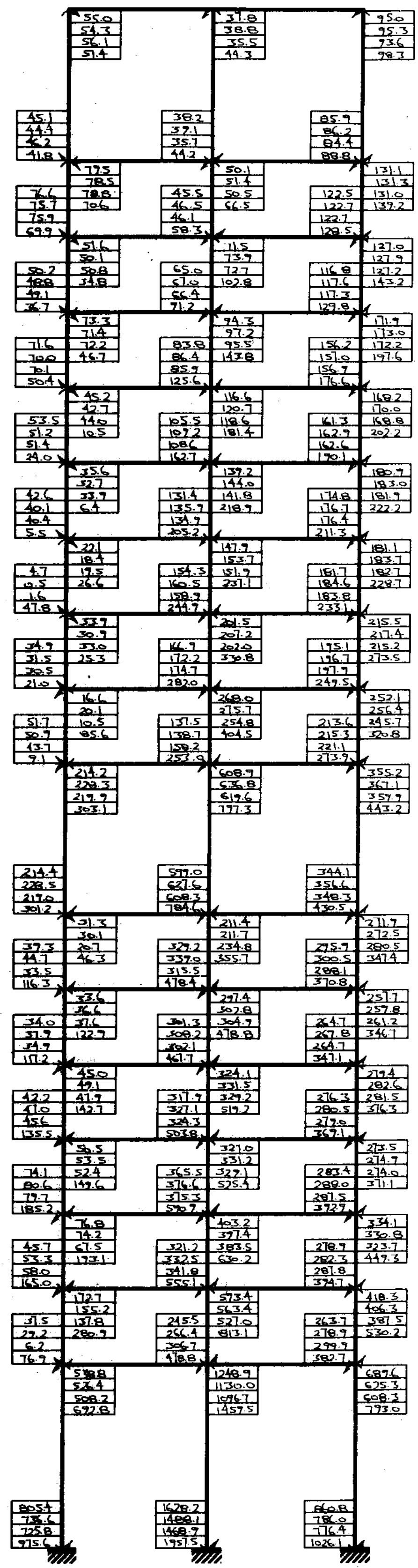

FIGURE A.10 FRAME TYPE TEN

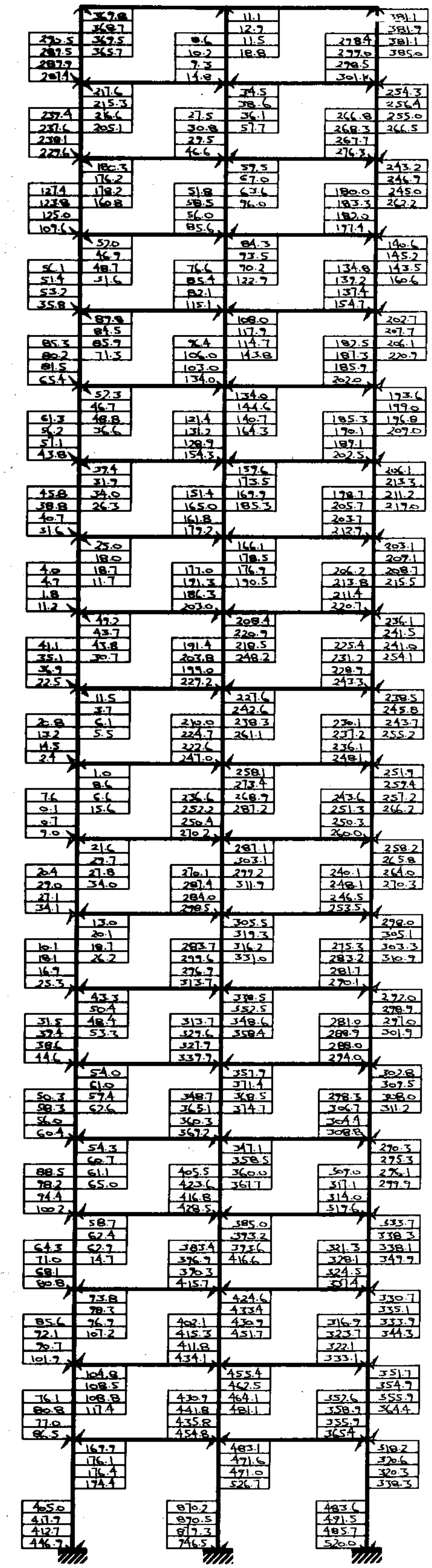

FIGURE A.11 FRAME TYPE ELEVEN